Vladislav Khayrudinov

Wireless Power Transfer System

Development and Implementation

Helsinki Metropolia University of Applied Sciences

Bachelor of Engineering

Information Technology

Thesis

31 March 2015

Helsinki Metropolia University of Applied Sciences

Author(s) Title Number of Pages Date	Vladislav Khayrudinov Wireless Power Transfer system. Development and Implementation. 57 pages 31 March 2015
Degree	Bachelor of Engineering
Degree Programme	Information Technology
Specialisation option	Embedded Systems and Electronics
Instructor(s)	Anssi Ikonen, Head of the Degree Programme Raimo Miettinen, COO, Nextfloor Oy

The goal of the project was to develop a Wireless Power Transfer (WPT) System and implement it in innovative flooring. The project was done at NextFloor Oy, a company based in Helsinki, Finland. At the moment, Wireless Power Transmission is in the forefront of electronics research, which is why this study started as an initial attempt to investigate WPT in order to keep up with the fast growing industry.

The main steps of the project were to study the physics behind wireless electricity transfer technologies, review the current industry situation and evaluate available solutions. Furthermore, the major objective included design of the printed circuit boards (PCBs), assembly and testing and development of original prototypes.

As a result, the system consisting of a transmitter and receiver boards, was developed. It utilizes the inductive coupling method in order to transfer electricity wirelessly. The unique prototypes, a Qi standard compatible demo-table and non-standardized wireless power floor-demo, were designed to work together with the NextFloor ingenious flooring system.

The goals were met and the 40 Watt Wireless Power Transfer System showed encouraging results. The primary part of this study was conducted during six months and further development and enhancements are carried out currently. The next essential phase includes the development of the 100-Watt WPT system and its laptop charging implementation and, finally, R&D of the magnetic resonance wireless energy transmission.

Keywords	wireless power transfer, inductive coupling, printed circuit board design, prototype development, electromagnetism

Contents

1 Introduction

Wireless power transfer (WPT) is an important topic nowadays. Although WPT has been known for more than a century, only now has the WPT industry started its rapid growth. The number of publications on wireless power has increased by at least 1200% in the last 10 years [9,2]. Current solutions are having great success in the marketplace with diffusions of innovations from innovators to early adopters as of now. However the main focus of the current solutions is a “wow” factor which in most cases neglects convenience [7,14]. Obviously, there is a need for a real-life application, for average users who are not particularly familiar with the engineering world and do not follow state of the art technologies.

The goal of the project was to evaluate and study the wireless power transfer technologies and physics behind it. The design and implementation of the wireless energy transmission system prototype and its implementation in the NextFloor innovative floor was the main plan. It was crucial for NextFloor to integrate advanced technologies into their floor system in order to make it really “smart” and innovative and wireless power transfer was one of them.

WPT is a very broad though relatively new technology – almost 80% of my references are dated later than the year 2010; hence, the scope of the project was limited to implementation of the inductive power transfer mode only. However, other types of WPT are also discussed in the thesis. The question my project was aimed to answer was simple: Are we ready to use cordless electricity in our everyday lives?

Last but not least, my utmost aims that I set in the beginning were to apply the gained knowledge in practice, assess my professional competence and development needs and learn how to work in a professional team researching a totally new technology.

2 Theoretical background

2.1 History of Wireless Power Transfer

The development of the WPT systems started already in the late 19th century with the ideas of Nikola Tesla, who is rightfully considered an acknowledged genius in this field [3, 1230]. Already then, he was rather skeptical about the slow though inevitable adoption of these technologies: “I shall proceed slowly and carefully… might not have been given to the world for a long time yet… my best wishes for your future success …see the excitement coming…” [1,1-4].

Tesla’s main idea was to use our planet as a conductor in order to transmit power to any point on Earth. As a result, he conducted successful experiments at Colorado Springs, Colorado in the 1900s, where a resonant transformer made of a 200 feet mast with a copper ball on top was built (the Tesla coil) [3,1231]. With frequency of 150 kHz and 300 KW of input power he was able to collect “thousands of discharges” up to 50 kilometers from the source, though there are no details of how much power was collected [1,2;3,1231]. Furthermore, Tesla’s Wardenclyffe tower, built on Long Island, was another sophisticated construction to pursue his goal of the World Wireless System. Unfortunately, this 154 feet high wireless power transmitter, which played a crucial role in Tesla’s inventions, was demolished a few years later due to his debts and the US Government claims that it acted as a spy transmitter [3,1231].

Brown (2011) states that the lack of technology, microwave power in particular, resulted in a continuous pause in development of wireless power until World War II when the first radars were made. Consequently, it boosted the point-to-point microwave transmission research. [3,1231]

As a result, William C. Brown’s cordless helicopter was introduced in 1964, the main concept of which was a 400W continuous power microwave transmitter delivering up to 100 W to the receiver end on the machine. [3,1231-1233.] Furthermore, as mentioned by Garnica et al. (2013) and Brown (2011), the idea of long-distance power transmission from space objects emerged where energy would be gathered, beamed from a solar-power satellite to Earth and then converted into electrical form. However, neither technique received any further attention in industry. [2,1322;3,1238.]

The next step towards WPT was development of the RFID system in 1973 where tags were powered using induction coupling. It took three decades before the WiTricity research group introduced the real cordless electricity transfer in 2007 with a 60W bulb being powered at two meters distance. Apparently, this was the starting point for a rapidly growing and competitive industry of wireless power transfer. [9,4.]

2.2 Main concepts of wireless transmission of electric energy

Every electromagnetic source creates both electric (**E**-fields) and magnetic (**H**-fields) fields around itself, and they are characterized by the radiative and non-radiative components. Depending on the distance from the source there are near-field, transition and far-field regions that are defined by the way they interact with the surrounding media. The small transition region has both the characteristic of near-field and far-field. [13,1.]

The situation when the distance to the source is less than $\lambda/2\pi$ is near-field (Figure 1). Near-field has a complex definition in terms of relation between **E** and **H**, but more importantly, it has all four types of polarisation present (horizontal, vertical, circular and elliptical), while far-field has only one type. [13,1.] A striking point is that a near-field region is a better environment for electromagnetic induction than far-field, where electric and magnetic fields decrease proportionally to the distance. [10,18.]

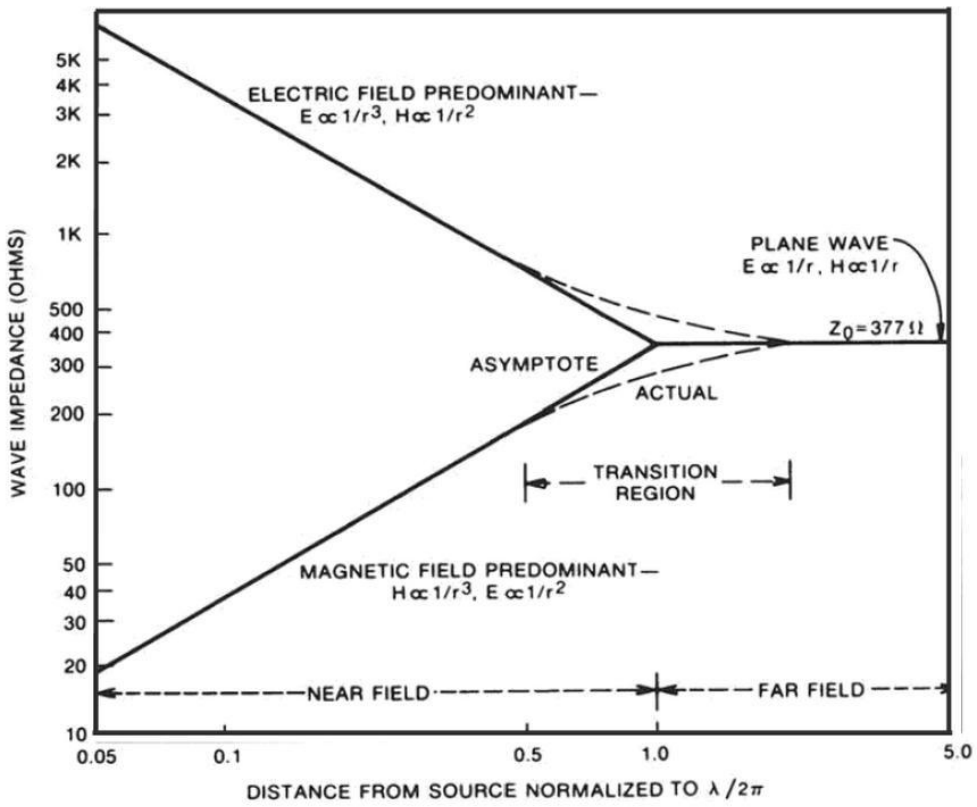

Figure 1. Free space wave impedance. Copied from Montrose et al. (2004) [10,18].

A near-field region allows higher power transfer efficiency and diffraction of the wave, which results in stronger penetrability and weak directivity on a short range. In addition, near-field transfer is divided into inductive (magnetic) coupling and capacitive (electrostatic) coupling. Capacitive coupling of two conductors is achieved via transfer of electric energy through dielectric media. However, inductive coupling is based on alternating magnetic field and considered to be more secure and productive for wireless power transfer. [9,5-6.] Figure 2 denotes the main WPT methods which were developed historically.

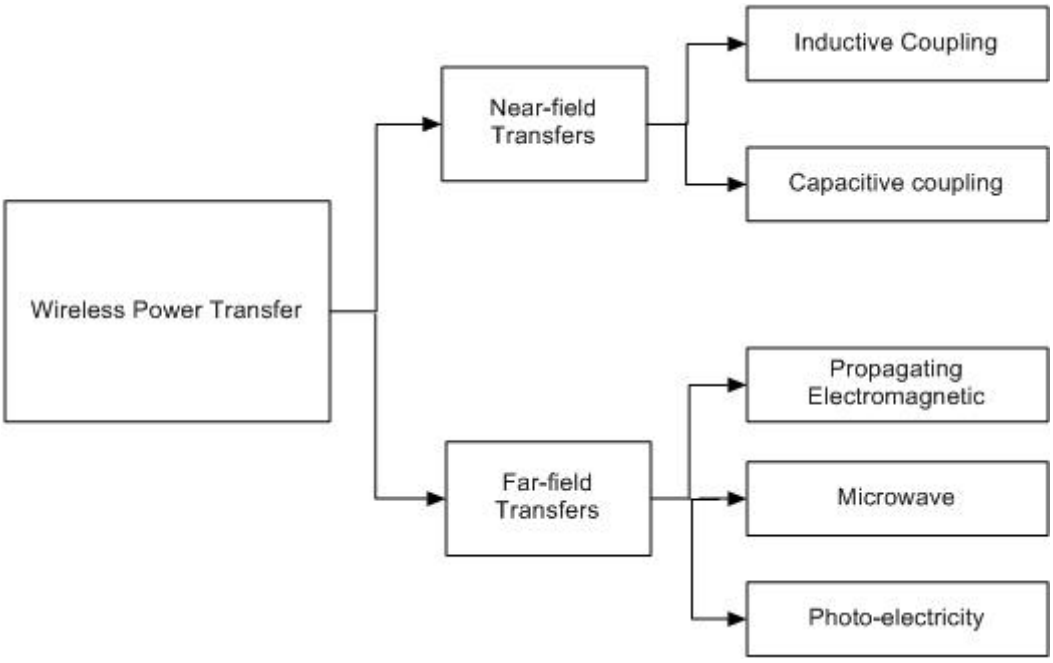

Figure 2. WPT types. Data gathered from Sun et al. (2013) [9,5].

Apparently, since far-field power transmission methods are not practical, due to weak penetrability, low efficiency and uncertain safety, the industry is more interested in the near-filed region. A typical near-field wireless power transfer system consists of several blocks (Figure 3). In most cases it is represented as strongly coupled primary power transmitter (TX) and secondary power receiver (RX) units separated by 1 to 10 cm. [2,1322; 9,5-18].

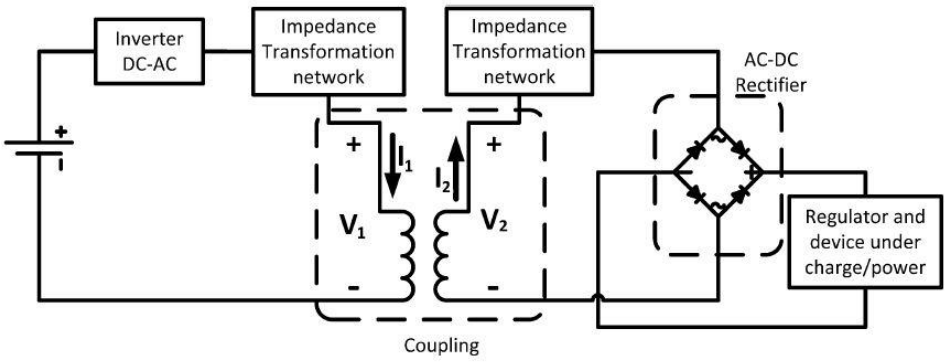

Figure 3. Typical near-field transfer system structure. Reprinted from Garnica et al. (2013) [2,1323].

The transmitter transforms DC to AC energy and couples it to the receiver via a coil or antenna. Firstly, there is a conversion from DC to AC at a set frequency (commonly

several hundred kilohertz) in the inverter unit, which is usually a high-efficiency switching circuit. This circuit especially plays a vital role on the transmitter side since it decides the overall efficiency of the system. Since the wavelength is relatively large compared to the distance between TX and RX, it is clearly a near-field system according to Figure 1.

The impedance transformation network represents the power management/tuning circuit, which essentially tunes transmitting power parameters according to the receiver's needs. Estabrook (2013) approaches communication between transmitter and receiver as either "in-band" or "out-of-band". In-band is implemented by using the same magnetic field for conversation as for power transfer. Small changes in amplitude or load modulation usually do it. Obviously, in that way the system is more reliable and easy to implement than out-of-band, which is most likely based on a Bluetooth connection between the TX and RX and requires separate power, more PCB area and higher cost. However, the out-of-band approach is efficiently used in loosely coupled systems. [9,125;7,13.]

Finally, AC energy is converted back to DC in a rectification circuit, which again plays a vital role on the receiver side since it decides the overall efficiency of RX.

2.3 Physics behind inductive coupling WPT

According to Oersted's law, a steady current produces a magnetic field around it [14,140]. Furthermore, Biot–Savart law describes the relation between the magnetic field and magnitude, direction, proximity and length of the electric current by which it was generated:

$$B = \frac{\mu_0}{4\pi}\int_l \frac{Idl \times e_r}{r^2} \quad (1)$$

where r is the full displacement vector from the current source to the field point, e_r is the unit vector of r, Idl is the infinitesimal current source point in the wire, μ_0 is the permeability of free space [9,18;14,140].

Let us suppose that we have two aligned coils separated by some distance in the near-field region (Figure 4). The magnetic field generated by TX circular coil at the point *x* (at RX coil) would then be:

$$B = \frac{\mu_{0NIa^2}}{2(a^2+d^2)^{3/2}} \quad (2)$$

where *N* is the number of wire loops, *I* is the transmitter inductor current, *a* is the radius of the TX coil, *d* is the distance between TX and RX [11,199].

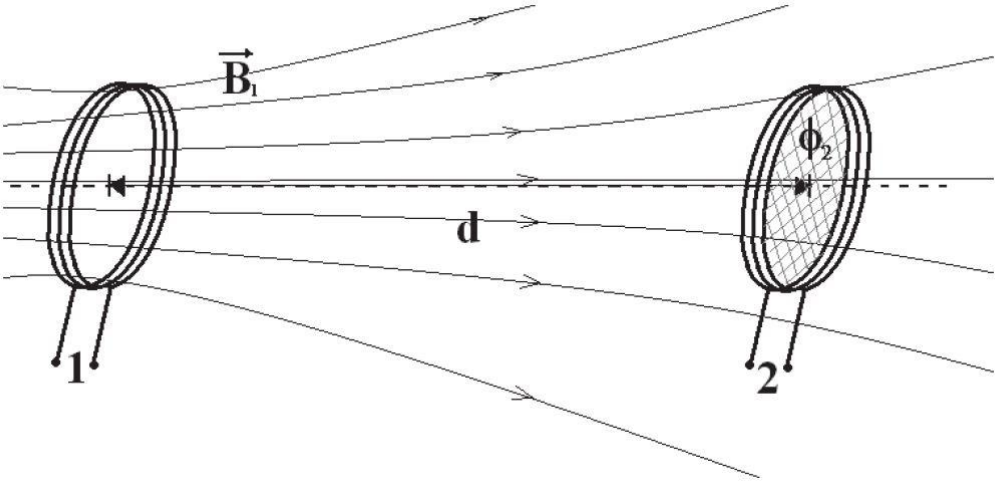

Figure 4. Magnetic field generated by transmitter coil crossing the receiver coil. Copied from Matias et al. (2013) [11,199].

The magnetic flux passing through the receiver will be expressed as:

$$\phi = \iint_S B\, dS \quad (3)$$

where *B* is the magnetic flux density generated by the transmitter and *S* is the area of the receiver coil surface [9.19]. Since the time-dependent current of the transmitter coil produces magnetic flux variation in the receiver coil, electromotive force (EMF) is induced in the RX coil, which we can derive by applying Faraday's law [14,166]:

$$\varepsilon = -\frac{d\phi}{dt} \quad (4)$$

where ϕ is the magnetic flux. The EMF is driving the current in the secondary coil whose magnetic field is opposing the time variation in the magnetic flux according to Lenz's law. Hence, the power is transferred from TX coil to RX coil. [14,169;9,14.]

Self-inductance is the property of the circuit when its own magnetic field is opposing the current change in the circuit. Self-inductance of the coil can be defined as:

$$L = \frac{N\phi}{I} \tag{5}$$

where N is the number of turns, ϕ is magnetic flux and I is the current of the coil [14,174]. By combining (4) and (5) we obtain:

$$\varepsilon = -L\frac{dI}{dt} \tag{6}$$

or

$$\varepsilon = -M\frac{dI}{dt} \tag{7}$$

where L is self-inductance of the coil, *M* is mutual inductance of two coils, I is the current of the coil. Obviously, the EMF induced on the coil is directly proportional to the self-inductance/mutual inductance of the coils and rate at which the current is changing. [14,175;9,21.] Another representation of mutual inductance is the following:

$$M = k\sqrt{L_1 L_2} \tag{8}$$

where *k* is the coupling factor, L_1 and L_2 are TX and RX inductances. The coupling factor defines the grade of the coupling, i.e. how much flux of the total flux actually penetrated the receiver coil. It can have a value from 0 to 1 (from zero to perfect coupling). [12.]

According to (2) and (3) and if the current is alternating, we retrieve:

$$\phi = \iint_A \frac{\mu_{0Ni\sin(\omega t)a^2}}{2(a^2+d^2)^{3/2}}\,dA \tag{9}$$

and combining with (4):

$$\varepsilon = -\frac{d(\iint_A \frac{\mu_{0Ni\sin(\omega t)a^2}}{2(a^2+d^2)^{3/2}} dA)}{dt} \quad (10)$$

or

$$\varepsilon = -\mu_{0Ni\omega\cos(\omega t)} \iint_A \frac{a^2}{2(a^2+d^2)^{3/2}} dA \quad (11)$$

which explains that the voltage induced to the secondary coil depends on the current/voltage in the primary coil, the frequency of the current/voltage in the primary coil, the distance between the coils and the surface area of the coils. The resulting two coil coupling system is depicted in Figure 5.

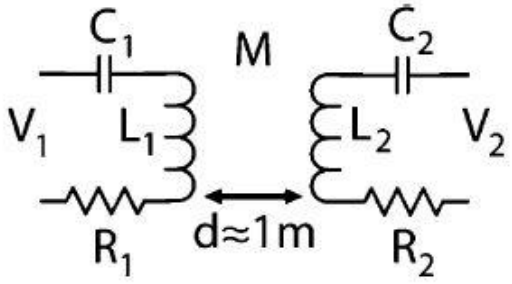

Figure 5. Simplified representation of the two coil coupling system. Reprinted from Garnica et al. (2013) [2,1326].

Here *C1* and *C2* are tuning capacitors, *L1* and *L2* are coupled inductors with mutual inductance *M, R1* and *R2* represent parasitic resistances (loss resistances in the inductors), *d* is the distance between the coils and *V1* and *V2* are input and output voltages. [2,1326;6,10.]

As stated both by Grajski et al. (2012) and Garnica et al. (2013), the output power of the second coil can be defined as:

$$P_{out} = \frac{{V_1}^2 \omega^2 M^2 R_L}{(R_1(R_{2+}R_L)+\omega^2 M^2)^2} \quad (12)$$

where ω is the operating frequency of the system, R_L is load resistance. The overall transmission efficiency is then:

$$\eta = \frac{\omega^2 M^2 R_L}{R_1(R_{2+}R_L)^2+\omega^2 M^2 (R_{2+}R_L)} \quad (13)$$

where the transmission efficiency η is defined as a ratio of input to output power. Thus the overall efficiency of the system depends only on the transmission frequency, mutual inductance, coils' parasitic resistances and load resistance.[2,1326;6,10.]

Q factor (Quality factor) is defined by the ratio of the inductance to the resistance of the coil. A higher Q factor means a lower energy loss and so better transmission efficiency. Usually Q factor has values from 0 up to 1000 for WPT coils. [12;9,44.] We define it as:

$$Q = \frac{\omega L}{R} \quad (14)$$

where L is the inductance of the coil, R is its resistance and ω is the operating frequency of the system. Obviously, Q factor increases when the operating frequency increases. However, when it reaches its peak values, it will decrease as the operating frequency continues to rise. What is more, a higher Q factor means a narrower bandwidth, which results in dropped coupling efficiency and the need of a tuning circuit. [12;9,44.] Now the maximum transfer efficiency is defined by Sun et al. (2013):

$$\eta = \frac{k^2 Q_1 Q_2}{(1+\sqrt{1+k^2 Q_1 Q_2})^2} \quad (15)$$

where k is the coupling factor between two coils, Q_1 and Q_1 are the quality factors of the transmitter and receiver coils. Consequently, in order to reach the maximum efficiency, developers should optimize the coupling and quality factors of their systems. [9,55.]

2.4 Health and safety considerations

Since WPT systems are based on the electromagnetic radiation, it is important to consider safety issues when dealing with cordless electricity transmission. Sun et al. (2013) states that there are still no official regulations or safety standards for WPT (which is another sign that it is a completely new industry) [9,32]. However, as claimed by the World Health Organization (WHO), developers can rely on the existing reference standards from the Institute of Electrical and Electronics Engineers (IEEE) and the International Commission on Non-Ionizing Radiation Protection (ICNIRP) [8,21].

There are two main standards nowadays: “IEEE Standard for Safety Levels with Respect to Human Exposure to Radio Frequency Electromagnetic Fields, 3 kHz to 300 GHz” (IEEE C95.1-2005) and “ICNIRP Guidelines For Limiting Exposure To Time-Varying Electric, Magnetic and Electromagnetic Fields (up to 300 GHz)”. According to Kesler (2013), although neither IEEE nor ICNIRP organisations have evidences to show that exposure to radio-frequency electromagnetic fields could cause cancer, they both agree that it could stimulate nerves and muscles, heat tissues and increase body temperature. Nonetheless, the existing limitations assure that the mentioned effects never happen if the device complies. [8,21.] Figure 6 summarizes both standards’ maximum permissible exposure of radio-frequency electromagnetic fields.

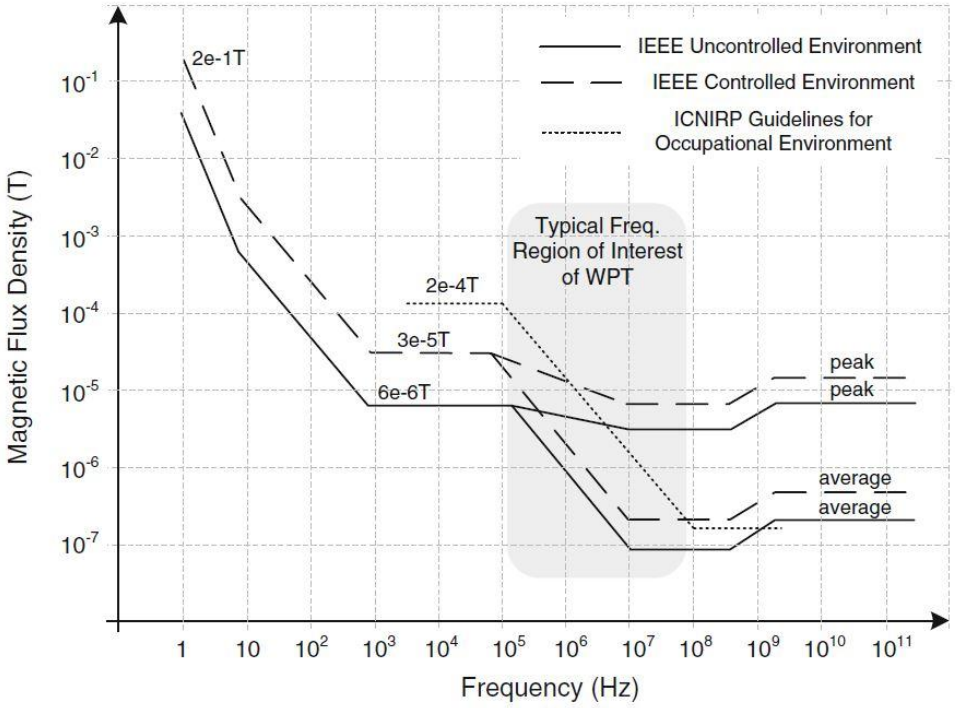

Figure 6. Maximum permissible exposure of radio-frequency electromagnetic fields proposed by IEEE and ICNRP. Copied from Sun et al. (2013) [9,34].

One point that clearly stands out is that the graph has a downward trend as the frequency goes up. Moreover, a typical WPT frequency range is denoted from roughly 100 kHz up to 100 MHz. The maximum permissible exposure is represented by three trends: IEEE controlled environment, IEEE uncontrolled environment and ICNIRP occupational environment. The IEEE controlled environment and ICNIRP occupational environment are less strict since they mean locations where people are aware of potential exposure while the IEEE uncontrolled environment is meant for the general public. [9,33.] Looking at the figure, we may say that a good rule of thumb could be that a 100 kHz system may have a maximum permissible exposure of 6 µT to certainly comply.

2.5 Main WPT interface standards and alliances

According to Pathare (2013), although the WPT industry is very young, already in 2012 more than 5 million WPT products were shipped, which is estimated to be 20 times more in 2015. Unfortunately, the standards “war” has already started with three main competing alliances: WPC, A4WP and PMA. Furthermore, every alliance is pushing its own complex incompatible technologies, specifications and designs. Hence, there is a

need for a universal, global standard (as was done with Wi-Fi) in order to ensure overall compatibility of the products, lower the costs and bust the innovation of this vast expanding field. [17.]

2.5.1 Qi by the Wireless Power Consortium (WPC)

The Qi standard is an inductive coupling power transfer interface standard developed by the Wireless Power Consortium (WPC). The Consortium was founded in 2008 as cooperation between European, American and Asian companies in different industries in order to develop a global standard for the inductive charging technology. The most prominent members include, for example, Motorola Mobility Inc., Microsoft Corporation, Nokia, ASUSTek Computer Inc., LG Electronics, Sony Corporation, HTC Corporation, TDK Corporation, Texas Instruments. [12.]

2.5.2 Rezence by the Alliance for Wireless Power (A4WP)

Rezence is a magnetic resonance power transfer standard developed by the Alliance for Wireless Power (A4WP). A single transmitter can power up to eight receiver devices on mid-range distances. Communication between transmitter and receiver is “out-of-band” and implemented via Bluetooth. The A4WP was founded in early 2012 in order to develop a ubiquitous WPT ecosystem. The most prominent members include Broadcom, Panasonic, Microsoft Corporation, LG Electronics, Samsung, Logitech, WiTricity, Qualcomm, Incorporated, Gill Electronics, Hewlett Packard, Integrated Device Technology, Inc., Intel and others. [15.]

2.5.3 Power Matters Alliance (PMA)

Power Matters Alliance (PMA) is a non-profit organization, which develops inductive and resonant power transfer standards. PMA was founded in 2012 in order to technically harmonize and advance multiple inductive WPT standards, promote WPT within the automobiles industry and popular public infrastructure venues. The most prominent members include Duracell Powermat, LG Innotek, Panasonic Corporation, Samsung Electronics, Toshiba Corporation, Sony Corporation, Energous Corporation, Freescale

Semiconductor Inc, Integrated Device Technology (IDT) and Microsoft Corporation. [16.]

Table 1. A summary of the main WPT Interface standards and alliances as of January 2015. Data gathered from Pathare (2013) et al [12;15;16;17].

Organization	WPC	PMA	A4WP
Established	2008	2012	2012
Number of members	203+	80+	140+
Transfer type	Inductive coupling	Inductive coupling	Magnetic resonance
Max. transfer power	5W (10-15W soon)	5W (10-15W soon)	up to 50W
Range	Short range	Short range	Mid-range
Transfer frequency	100 to 205 kHz	277 to 357 kHz	6.78 MHz
Latest version	1.1.2	PMA1.1	A4WP-S-0001 v1.2
Certified Products	684	24	-
Authorized test labs	10	3	2

On CES 2015, the Alliance for Wireless Power (A4WP) and the PMA announced that they have agreed to merge into one organization with the intent to create a unified standard, which was already criticized by WPC representatives [15]. Apparently, there is a positive trend towards a global WPT standard although now the standards “war” will continue between A4WP+PMA and WPC.

2.6 Wireless power market overview

According to Sanderson (2014), the Wireless Power Market will have a steady growth up to $8.5 billion in 2018 (Figure 7).

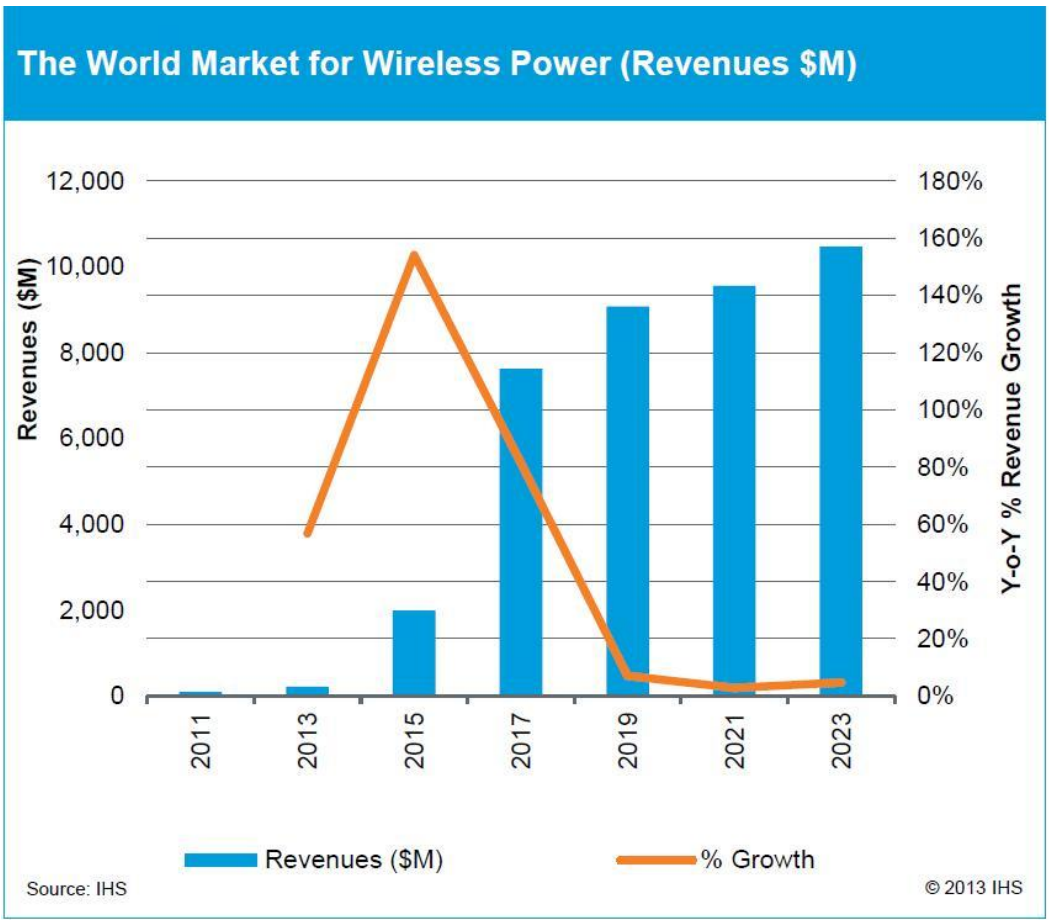

Figure 7. The world market for WPT. Copied from Sanderson (2014) [18].

Interestingly, IHS Technology forecasts the possible mergers and partnerships between alliances in 2015 (justified by the recent A4WP+PMA merger), which will certainly boost the industry with a significant increase to the year 2017 [18].

What is more, Balouchi et al (2012) states that the market will gain a considerable push in different applications from major industry players such as the Institute of Electrical and Electronics Engineers, PMA, WPC, A4WP, Google, Facebook and General Motors. (Figure 8) [19.]

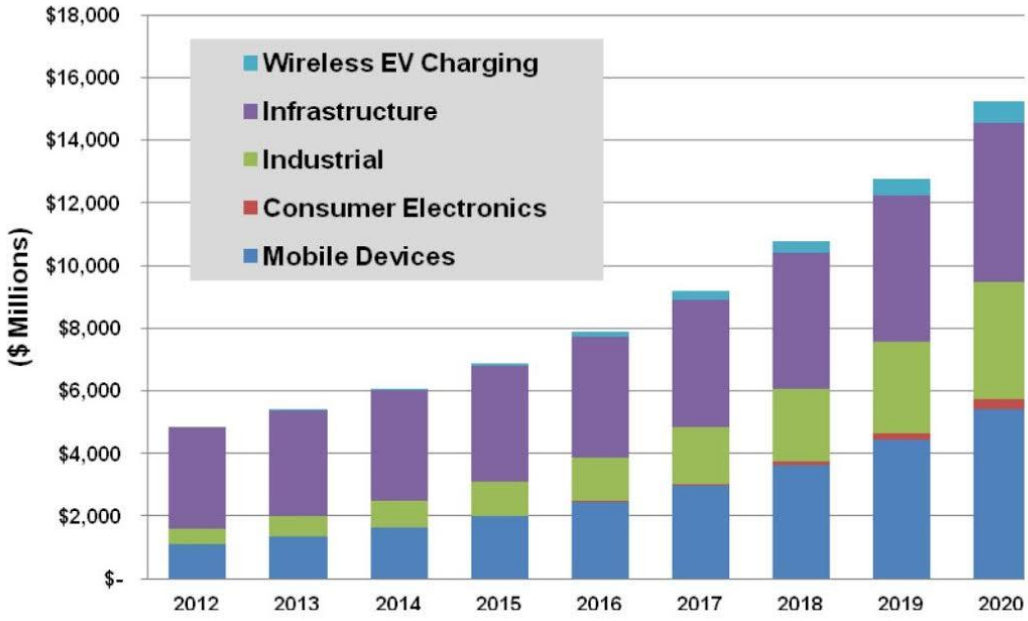

Figure 8. Wireless Power revenue by application. Copied from Balouchi et al (2012) [19].

It is true to say that the biggest revenue will be from infrastructure and industrial applications and mobile devices. However, we will see a gradual rise of consumer electronics and wireless electric vehicles charging sectors as the technology develops further.

Furthermore, Balouchi et al (2012) forecasts that the Asia-Pacific region's revenues will eventually surpass the North America region having 40% versus 27% share in 2020 (Figure 9).

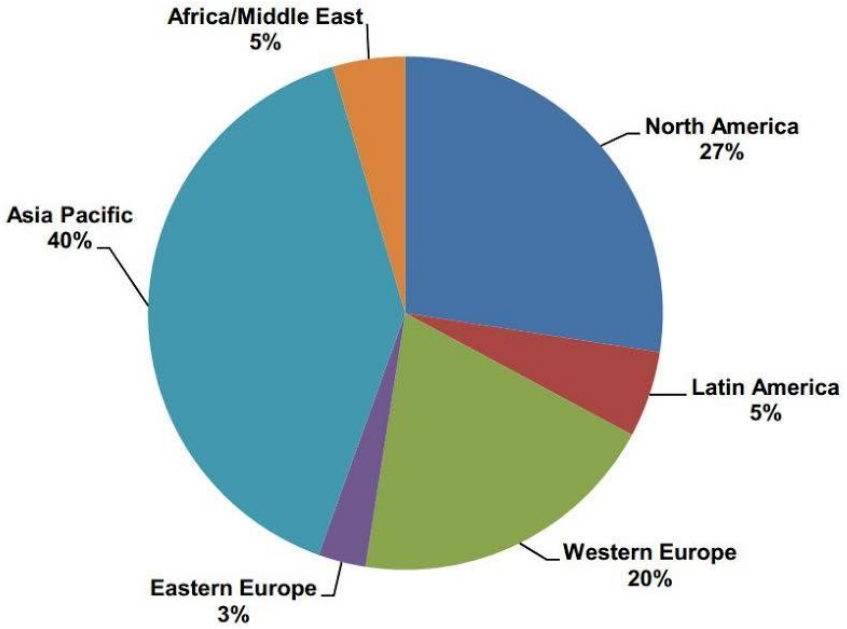

Figure 9. Wireless Power revenue share by regions in 2020. Reprinted from Balouchi et al (2012) [19].

Apparently, the Western Europe market will have a third biggest share with 20% leaving Africa/Middle East and Latin America behind.

Most interestingly, Balouchi et al (2012) proposes that the biggest trend for the next few years will be a steady decline of induction coupling power transfer type from 80% to 10% and, at the same time, a steady grow of magnetic resonance applications from 0% to 72% until 2020 (Figure 10).

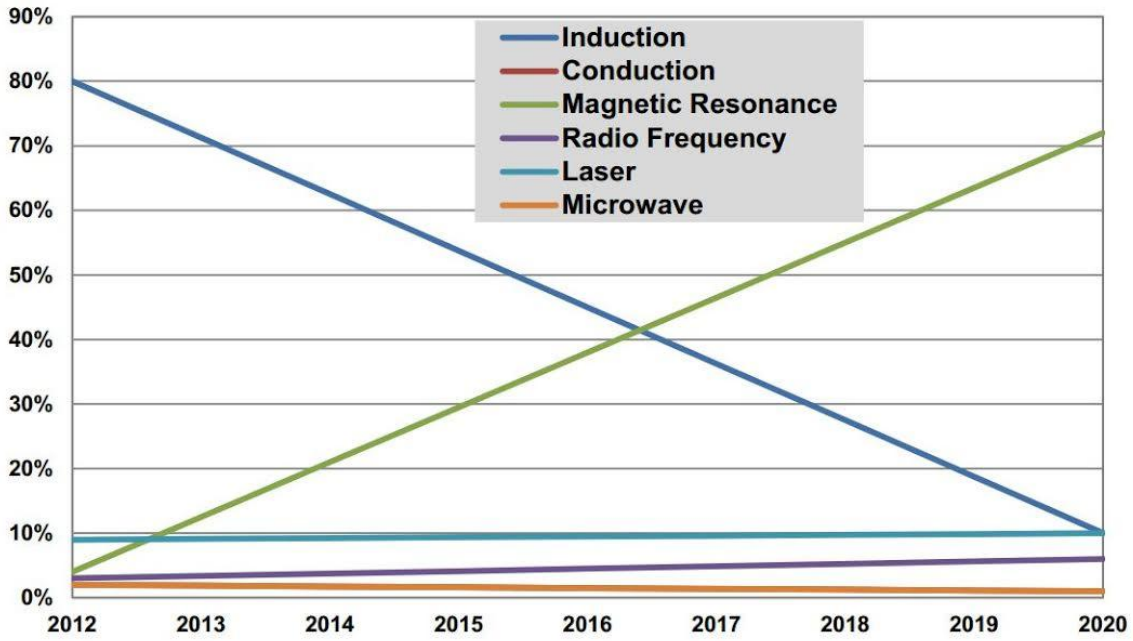

Figure 10. Wireless power share by technology. Copied from Balouchi et al (2012) [19].

The most persuasive argument in favour of the magnetic resonance technology is that it allows more alignment freedom, better range and multiple-device charging. Obviously, magnetic resonance (or a combination of two) is the future of WPT. However, nowadays, inductive coupling transfer is in the centre of attention with only a few if any magnetic resonance solutions on the market. Interestingly, the share of other WPT types (microwave, laser etc.) will have almost no growth at all due to its far-field nature limitations.

3 Methods and materials

3.1 Texas Instruments Qi compliant modules evaluation

It was reasonable to begin the WPT technology research and development with evaluation of existing products on the market. Nowadays, Qi standardized 5W transmission systems were the only products officially manufactured according to Qi regulations. Such companies as Texas Instruments, IDT, and Triune Systems produce similar evaluation kits based on inductive coupling WPT. We decided to evaluate the state-of-the-art evaluation kit from Texas Instruments.

TI 5W EV kit consists of two boards, which are a transmitter (TX) and a receiver (RX). TI BQ500210EVM-689 (Figure 11) is a single channel WPC certified transmitter, which provides a maximum output of 5W (19V input, 5V output). It has a common layout for transmitter boards where electronic components are located on the left side and a coil with ferrite occupies the right side of the PCB. [20.]

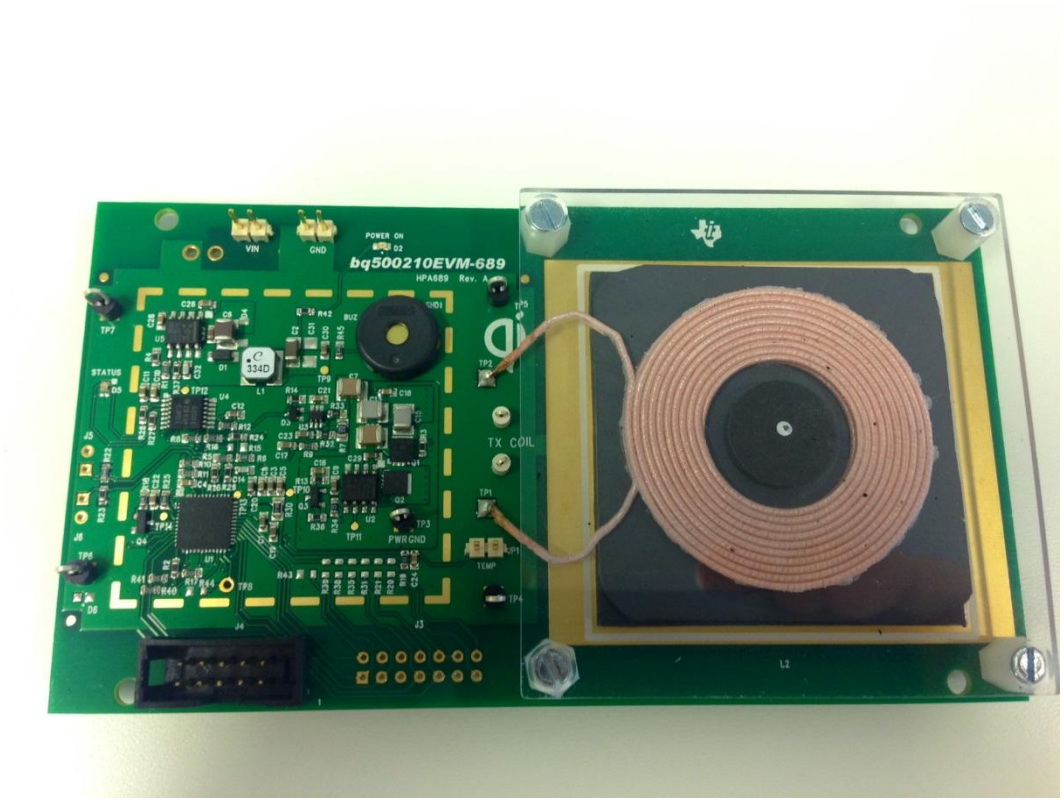

Figure 11. TI BQ500210EVM-689 transmitter module.

TI BQ51013AEVM-765 (Figure 12) is a receiver module which is mainly to be used with low-power battery devices. The output voltage is 5V up to 1A. Although the TX module has a standard for the WPT coil, the receiver has a thin low-profile coil. [20.]

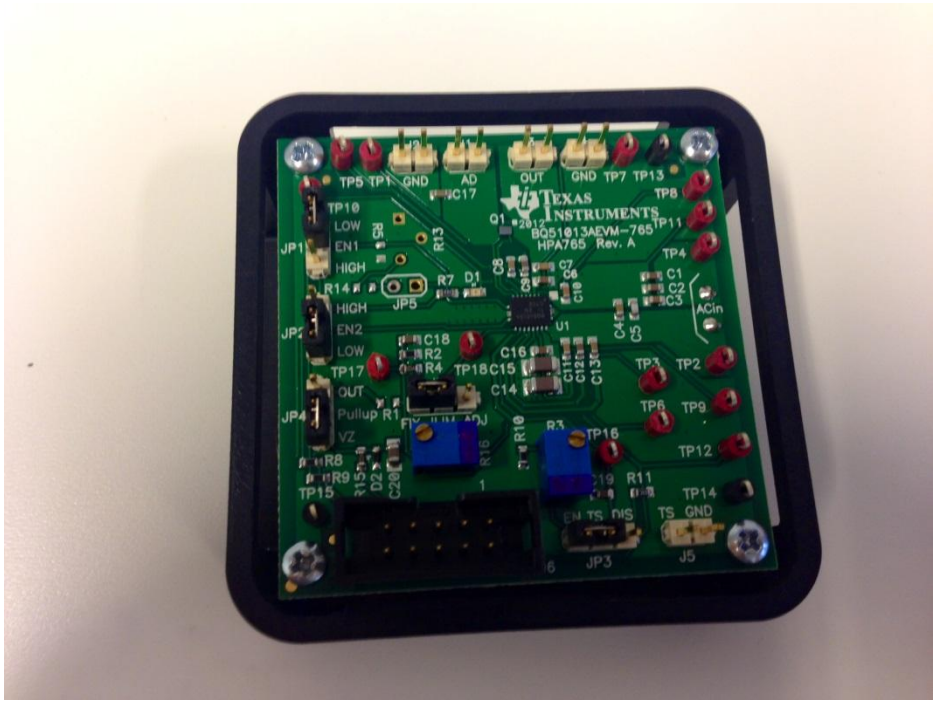

Figure 12. TI BQ51013AEVM-765 receiver module.

In order to fully evaluate the system, thorough schematic/layout documentation studies and a number of tests were done during the proof-of-concept stage of the project (Figure 13).

In particular, the effect of the length of the coil's wires was tested which showed that wires up to 4 meters (at least AWG size 9) can be used without major efficiency degradation. It could be very useful since it is not always convenient to have a transmitter right below its coil, rather than at a centralized control unit.

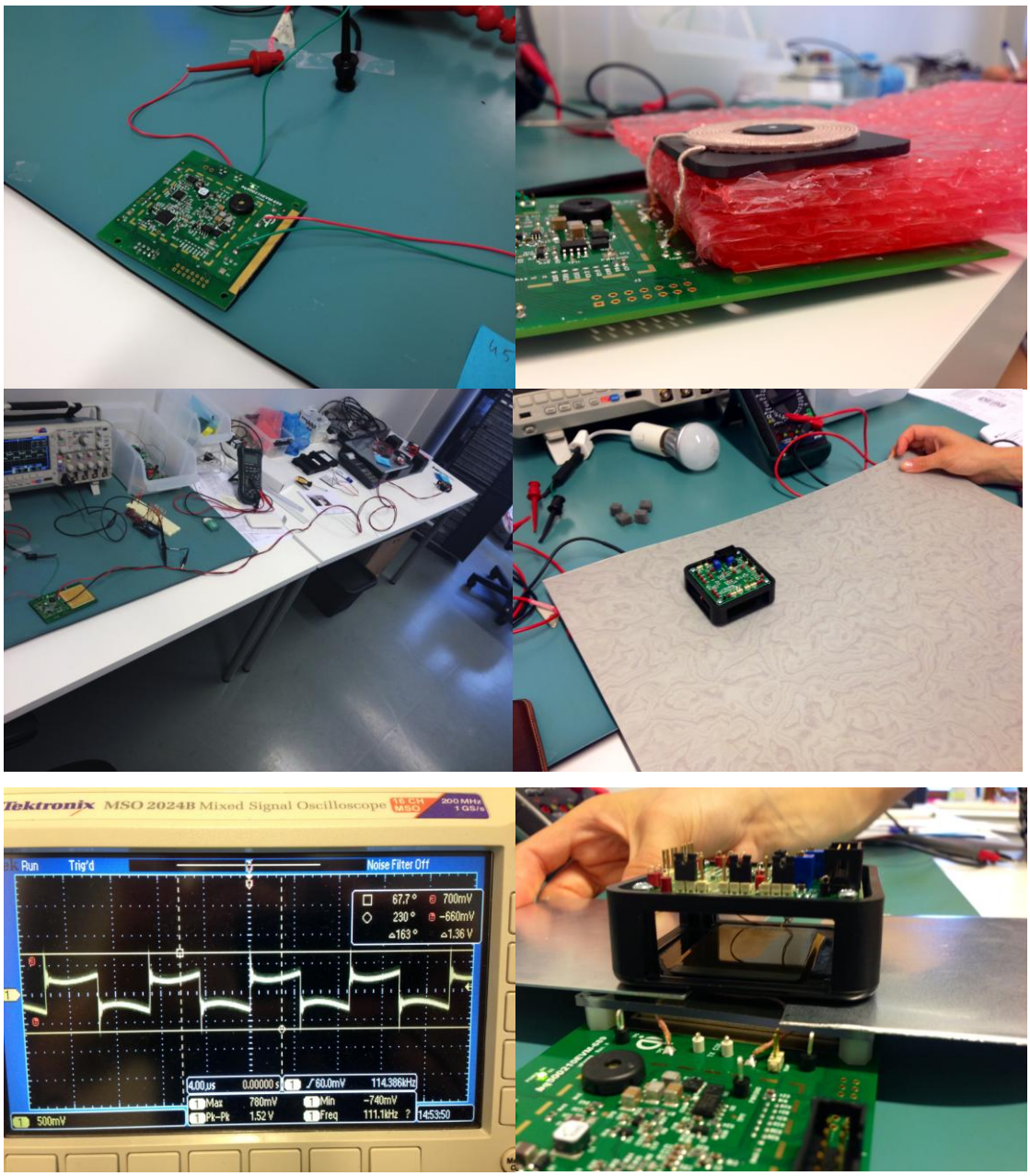

Figure 13. TI 5W Qi kits evaluation and testing.

Furthermore, different flooring materials were placed between the transmitter and receiver. The maximum thickness of 5 mm was achieved with no load. Also the metal detection mechanism was checked and it appeared that at least a 25 mm window between the metal plates was required to provide reliable transmission (Figure 13).

It has to be said that one of the most important characteristics is transmission efficiency. The measurements data is presented in Table 2 and the corresponding efficiency curve is presented in Figure 14.

Table 2. TI 5W Qi kits efficiency measurements data.

TX voltage, V	TX current, A	TX power, W	RX power, W	Efficiency
19	0,093	1,767	0,5	28,29654782
19	0,112	2,128	1	46,9924812
19	0,129	2,451	1,5	61,1995104
19	0,155	2,945	2	67,91171477
19	0,183	3,477	2,5	71,90106414
19	0,218	4,142	3	72,42877837
19	0,252	4,788	3,5	73,0994152
19	0,29	5,51	4	72,59528131
19	0,328	6,232	4,5	72,20795892
19	0,366	6,954	5	71,90106414

The test was done using Array 3711A (300W) (0~360V DC), which is a single input programmable DC electronic load. TX voltage is the voltage supplied to the transmitter module and RX power is the total power that sinks in the load on a constant current mode.

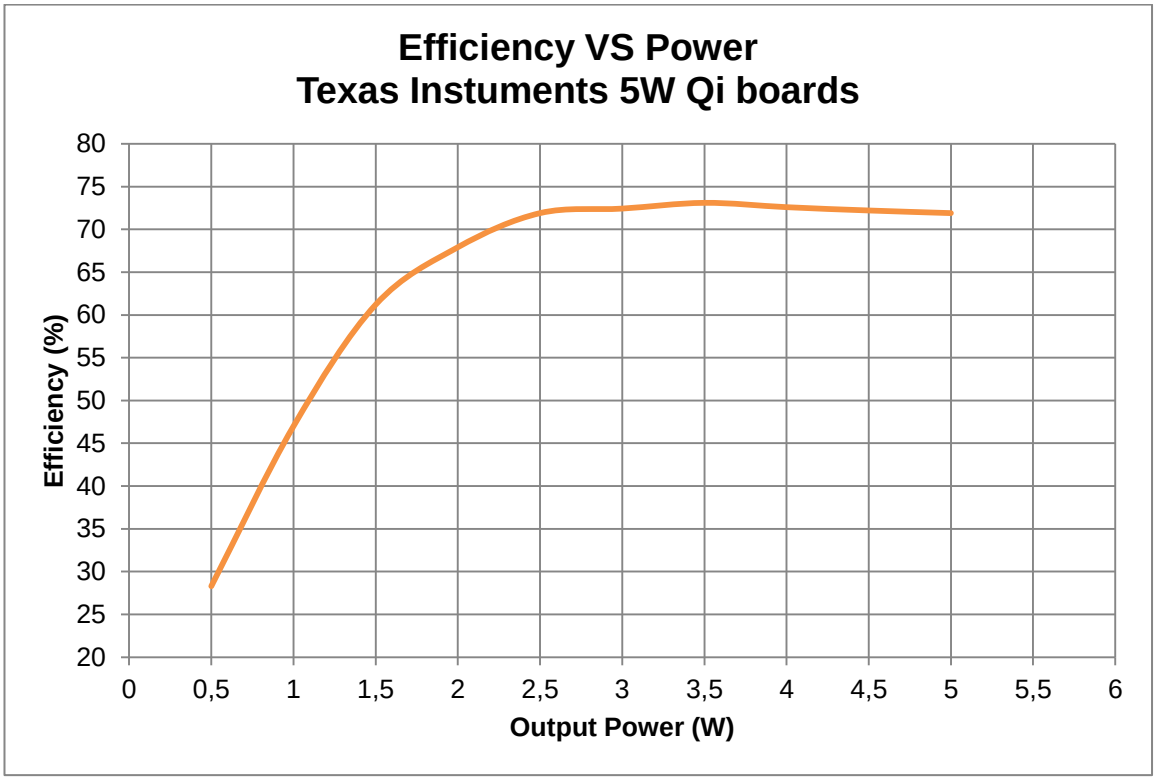

Figure 14. TI 5W Qi kits measured transfer efficiency curve.

As can be seen from the graph the efficiency rises drastically but exceeds 70% only after ~2.25 W. In addition, the maximum achieved distance is 5 mm through different floor materials including linoleum, carpet and rubber.

The system was proven to be working as expected. However, a strict limitation to maximum of 5 W power output, tight alignment of the coils and too short range (only up to 1 cm) were the main drawbacks. They prevented the system from being “truly wireless” and provide a considerable advantage over traditional wires. A better solution was needed.

3.2 NextFloor custom 40W WPT system

Despite the availability of the 5W Qi standard technology, we were interested in powerful solutions, which were not available on the European market. We started to search for those on the Asian market and succeeded in finding a company in Taiwan, which provided us with a reference system and technology support. After proving the reliability of the concept and evaluating the system, we proceeded with the design and development of PCBs and implementation of a custom 40W wireless power transfer system.

WPT development included several steps:

1. PCBs schematic design
2. PCBs layout design
3. Bill of materials (BOM)
4. Components order
5. PCBs manufacturing
6. Assembly and soldering
7. Testing and debugging
8. Development of the prototypes

3.3 PCB schematic design

3.3.1 Transmitter schematic

The schematic design was done in PADS DxDesigner, which is a part of Mentor Graphics PADS ES Suite (version 9.5). The principal schematic of the transmitter module can be divided into 4 parts. The input power circuit module is shown in Figure 15.

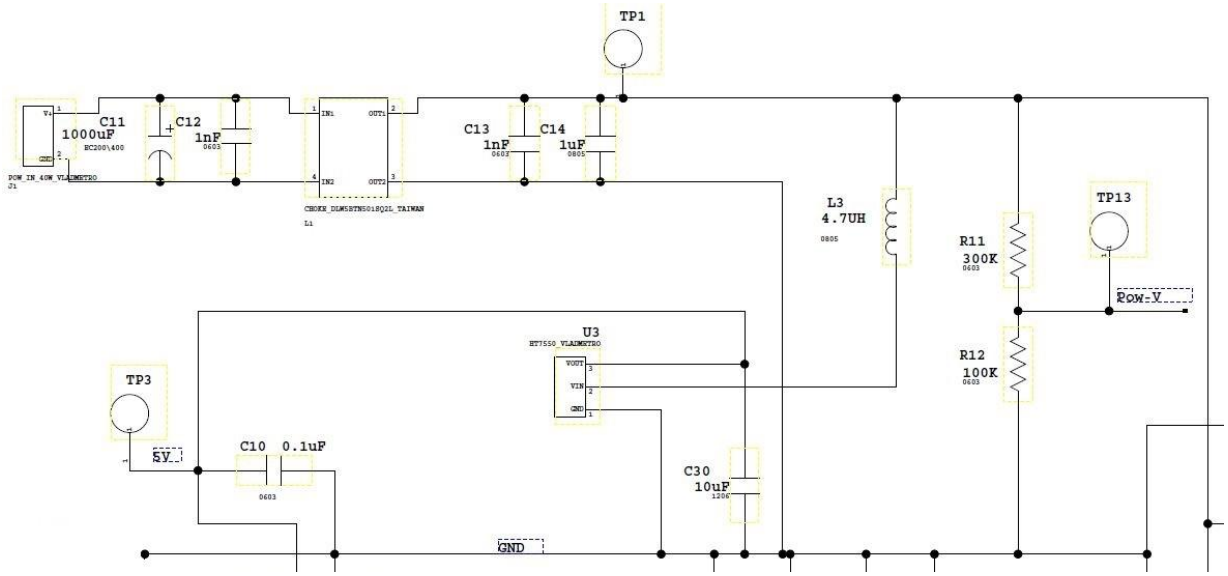

Figure 15. Input power schematic part.

The input power (12V) is supplied via connector J1. Then undesired frequencies are removed by capacitor-input filter (C11-C14 capacitors and L1 high current common mode choke). Then the ripple components are further removed by L3 inductor and the supply is fed into a U3 low-dropout regulator (LDO) which supplies 5V for the microcontroller (MCU) and other components. C30 10uF decoupling capacitor improves transient and noise performance of the LDO. The resistors divider (R11 and R12) is used by POW-V pin of the MCU for inspecting the operating voltage in order to adjust the primary sensing voltage of the receiver.

Figure 16 illustrates the MCU control circuit module. TPA parts represent test points. LED1-4 are transmission control indicators.

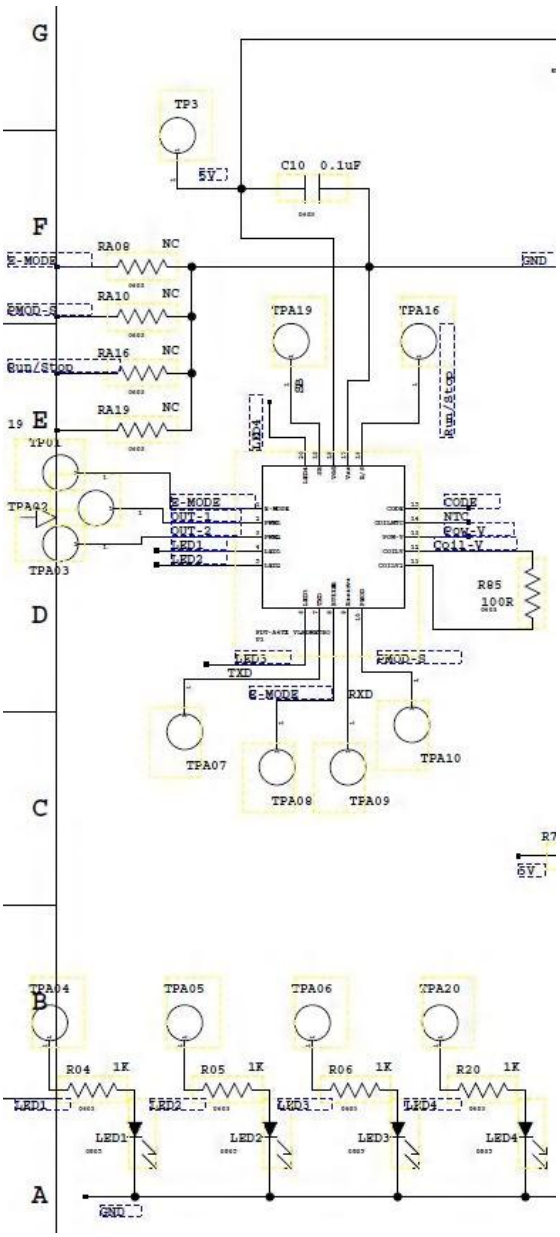

Figure 16. MCU control schematic part.

The transmitter's MCU is a 20-pin (QFN20) microcontroller designed especially for WPT applications. Its typical operating voltage is 3.5-5.5V with 0.3-1mA supply current in standby and 12-15mA in the operation mode. The pins' names and their functions are clarified in Table 3.

Table 3. Transmitter MCU pin functions.

Pin number	Name	Type	Function
1	E-MODE	Input	Operation setting
2	PWM-1	Output	Driving source 1
3	PWM-2	Output	Driving source 2
4	LED-1	Output	Failed operation indicator
5	LED-2	Output	Metal detection indicator
6	LED-3	Output	Operation status indicator
7	TXD	Output	UART Port to link with PC
8	BUZZER	Output	Buzzer driver
9	Reserve	-	Reserved
10	PMOD-S	Input	Factory setting
11	COIL-V2	Input	Detect coil voltage
12	COIL-V	Input	Detect coil voltage
13	POW-V	Input	Inspect operating voltage
14	COIL-NTC	Input	Over temperature protection
15	CODE	Input	Response signal from receiver module
16	R/S	Input	Run/Stop mode
17	Vss	Input	Negative supply voltage (Ground)
18	Vdd	Input	Positive supply voltage
19	SB	Input	For battery use
20	LED-4	Output	Receiver status indicator

The divider circuit mentioned above sets the POW-V pin to around 1-4V in order to inspect input power. If the input power is higher than the maximum voltage or lower than the minimum voltage, the system will stop its operation and LED1 will turn on. Pins PWM-1 and PWM-2 are inverse phase signals, which drive the DC-AC converter circuit. Pins COIL-V and COIL-2 are used to detect voltage from the coil and optimize PWM-1 and PWM-2 accordingly to keep the operation.

The DC-AC converter circuit module is represented in Figure 17. It is a Class D inverter/amplifier circuit where two power MOSFETs are used as switching devices.

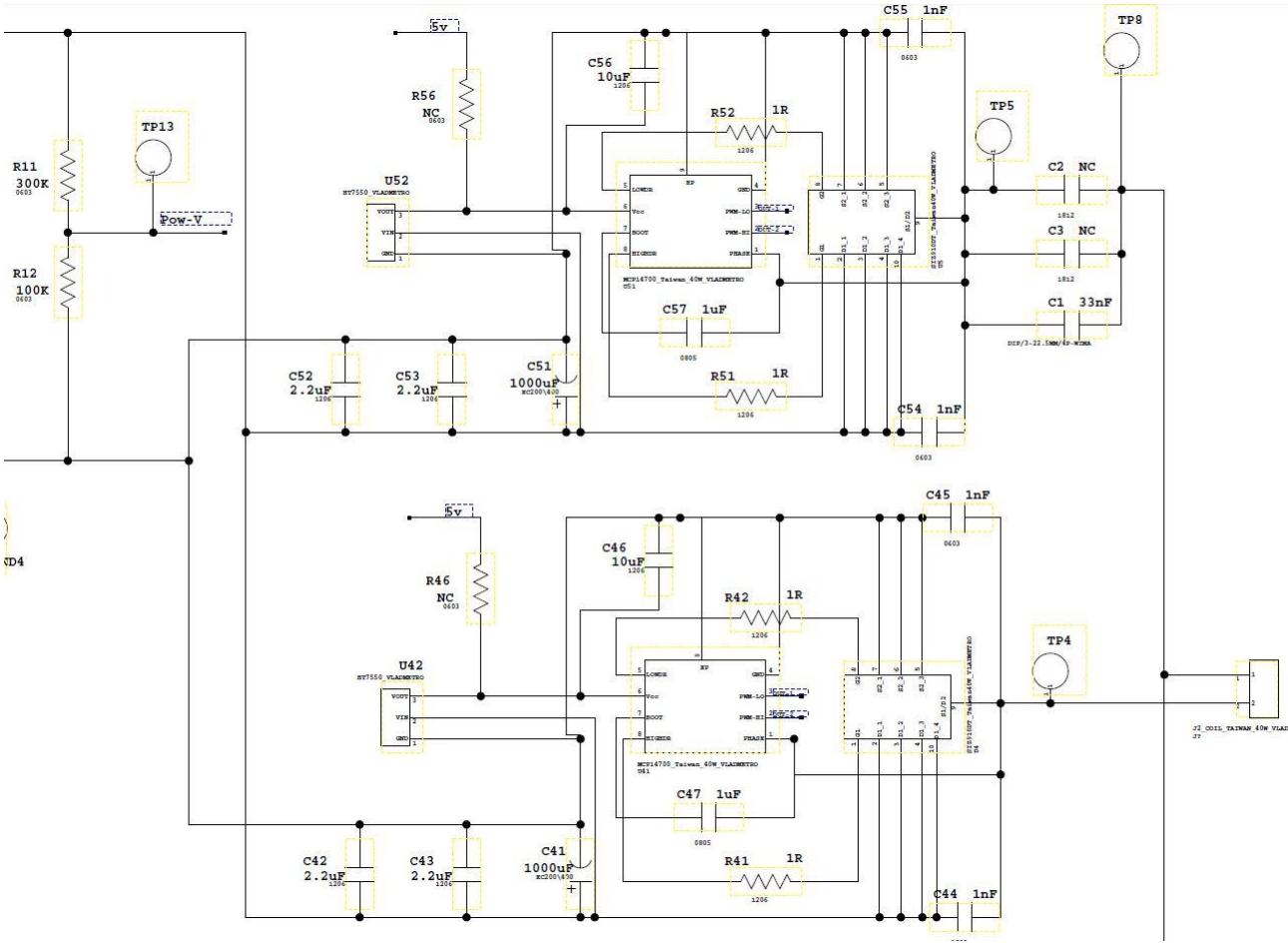

Figure 17. DC-AC converter schematic part.

The inverter is controlled by PWM-1 and PWM-2 pins of the MCU, which provide inverse phase 125 kHz signals to U41 and U51 MOSFET drivers (Microchip MCP14700). MOSFET drivers accept a low-power input from MCU and produce a high-current drive input for the high side and low side U4 and U5 N-Channel MOSFETs (Vishay SIZ910DT-T1-GE3). Without drivers the switching would be too slow and there would be a current overdraw in MCU, which causes overheating and leads to its permanent damage. The drivers are powered by U42 and U52 5V LDOs. Dual N-Channel MOSFETs have maximum Drain-Source Voltage of 30V, Gate-Source Voltage ±20V and Continuous Drain Current of 40A. Each MOSFETs outputs 125 kHz 12-14Vp-p square wave signal which then results in 125 kHz 24-28Vp-p single on the TX coil (connector J2). C1-C3 (0.22uF) are resonant capacitors tuned to fit 12uH transmitting coil.

The tuning circuit module is shown is Figure 18. It is implemented in such a way that the feedback from the transmitter itself is used to adjust the AC voltage magnitude in-

dependently from the receiver side. The voltage of the transmitting coil is constantly measured by the power monitor in order to keep it as high as possible and to adjust the frequency if necessary.

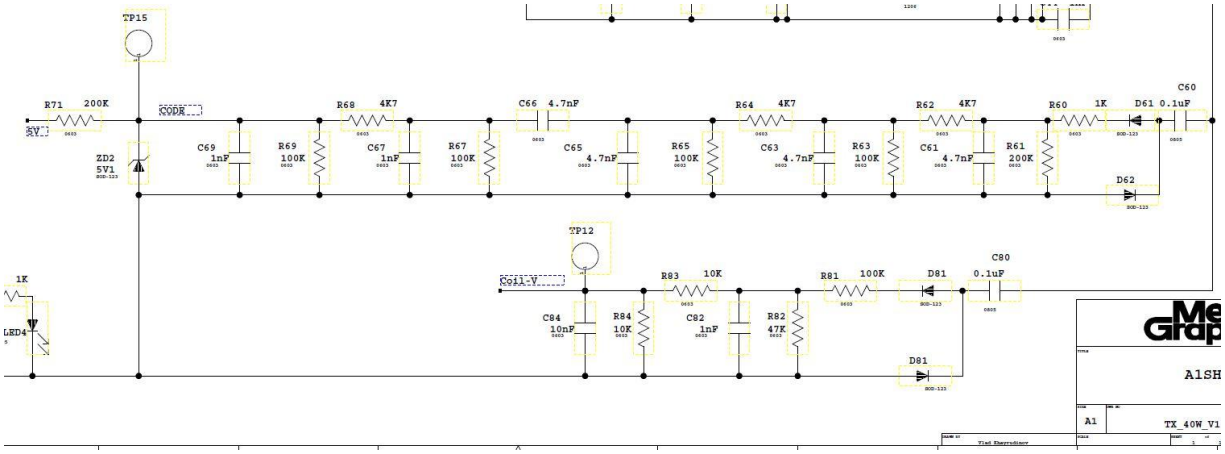

Figure 18. Tuning circuit schematic part.

The transmitting coil is connected to COIL-V and COIL-V2 pins of the MCU via the filtering network. They are used to detect the DC voltage from the resonance coil and optimize PWM-1 AND PWM-2 to keep the operation. Another filtering network connects the transmitting coil to the CODE pin of the MCU to obtain the response signal from the receiver and detect the location and existence of the receiver.

3.3.2 Receiver schematic

The principal schematic of the receiver module can be divided into 5 parts. The AC-DC converter (rectifier) and feedback circuit modules are shown in Figure 19. It is the most important part of the receiver since the overall efficiency of the module is defined by the rectification of the induced AC voltage.

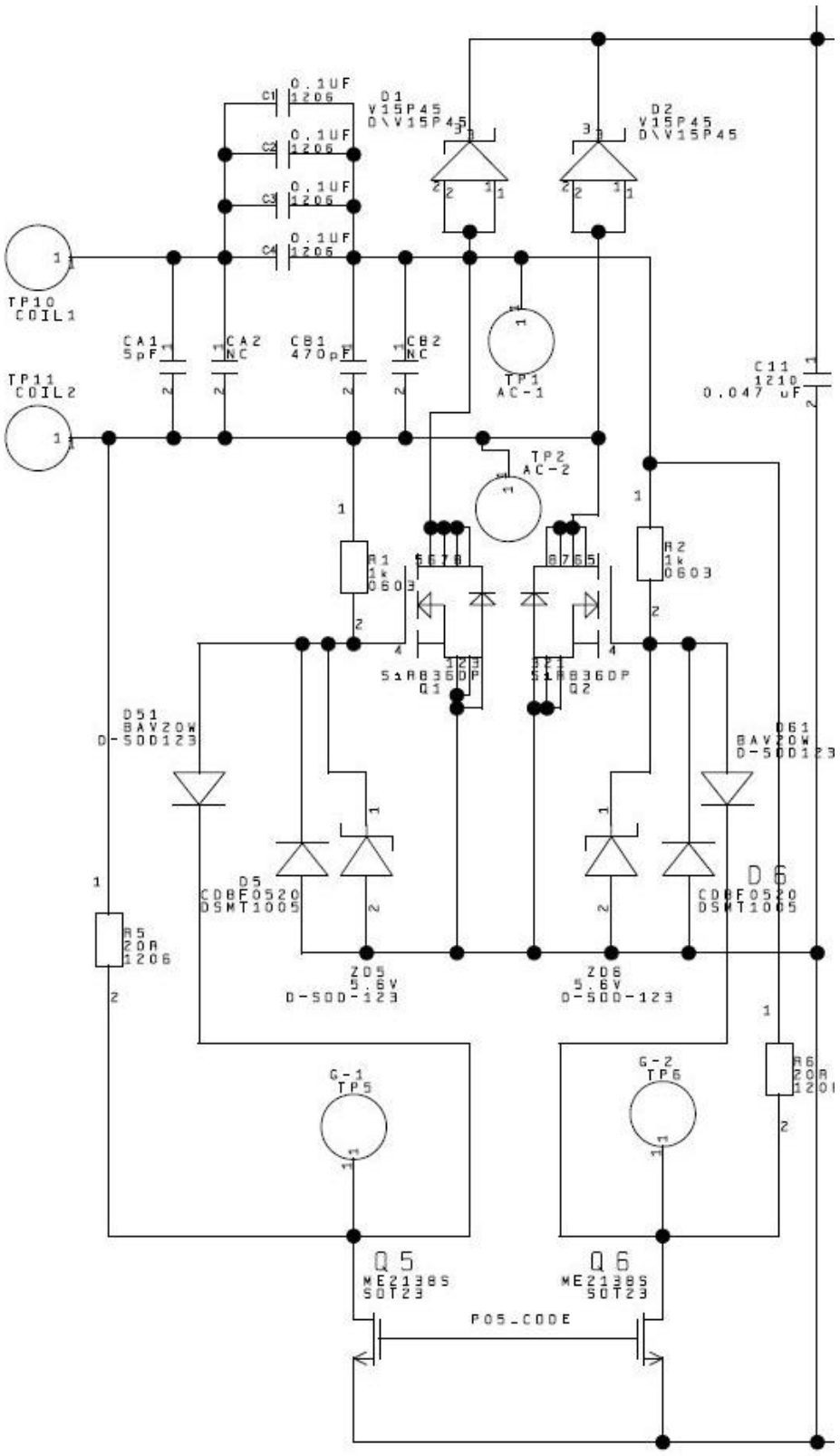

Figure 19. AC-DC converter and feedback schematic part.

The AC-DC converter is actually a half-bridge synchronous rectifier that eliminates a major disadvantage of the diode rectifier, which is an inevitable forward voltage drop of the diodes. The alternating current induced on the receiver coil is rectified without addi-

tional control from MCU by means of two Q1 and Q2 N-Channel MOSFETs (Vishay SIR836DP-T1-GE3). Zener diode clamps ZD5 and ZD6 are limiting the gate voltage on each MOSFET to 5.6V.

During the positive half-cycle the current goes from a positive output of the coil through the resonant capacitors C1-C4 then via the D1 TMBS diode (Vishay V15P45-M3/86A) then further towards voltage the detection unit and DC-DC (buck) converter. The high voltage potential created by the coil establishes a power loop via resistor R2, a closed gate terminal of the Q2 to negative output of the coil. During the negative half-cycle the current goes from negative output of the coil through the resonant capacitors C1-C4, then via the D2 TMBS diode (Vishay V15P45-M3/86A) then further towards the voltage detection unit and DC-DC converter. The high voltage potential created by the coil creates a power loop via resistor R1, the closed gate terminal of the Q1 to positive output of the coil.

The feedback circuit consists of Q5 and Q6 N-channel enhancement mode MOSFETs (Figure19) which are controlled directly by the receiver's MCU (Pin CODE). By switching both gates at the same time, the MCU can transiently break off the transmission by grounding the current path and thus discharging the capacitor C11 and charging it again ,as a result, increasing the amplitude of the load for a moment and in this way feeding back the data signal to the transmitter unit without power loss.

The voltage detection module is shown is Figure 20. The rectified signal is detected after R11 and R12 resistor divider circuit by pin V-D of the MCU and it outputs feedback according to the input voltage (Pin CODE). The connection to the DC-DC converter circuit is controlled by pin Pow-SW that acts as a circuit breaker.

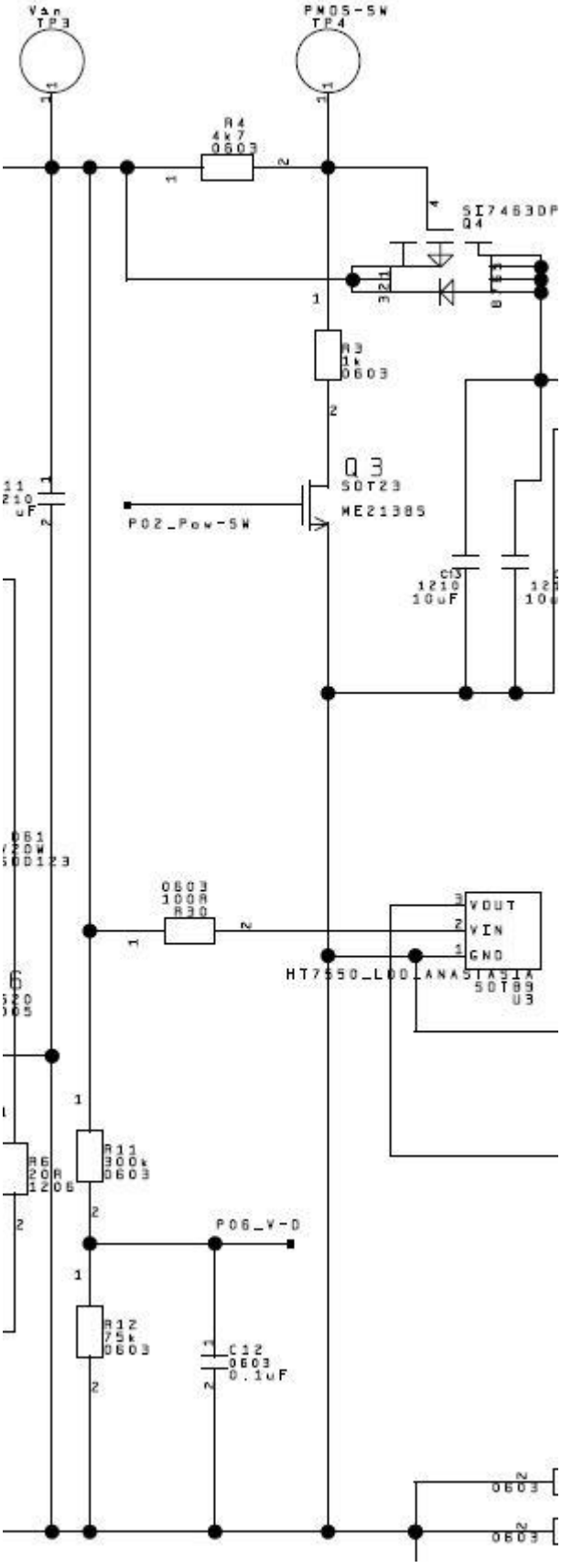

Figure 20. Voltage detection schematic part.

During normal operation, the gate of the Q3 N-Channel MOSFET (Diodes Incorporated ZXMN2A14FTA), connected to pin Pow-SW, is high and the gate of the Q4 P-Channel MOSFET (Vishay SI7463DP-T1-E3) is low, so the rectified current flows into DC-DC converter. If the V-D detected voltage is out of range, then the MCU pulls pin Pow-SW low, which turns off Q4 and the connection to the step down converter breaks.

Figure 21 represents the MCU control circuit module.

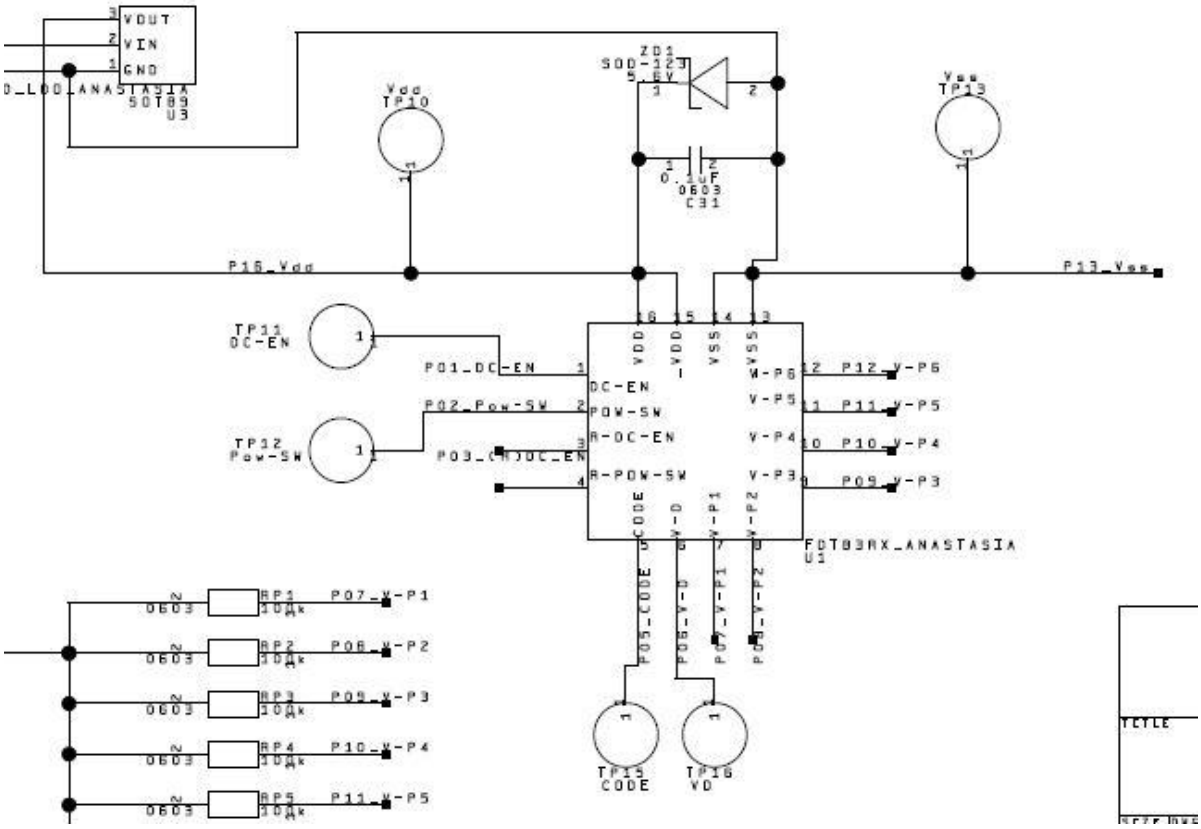

Figure 21. MCU control schematic part.

The receiver's MCU is a 16-pin (QFN16) microcontroller designed especially for WPT applications. Its typical operating voltage is 4.5-5.5V with a 1.5-2mA supply current in the operation mode. The pins' names and their functions are clarified in Table 4.

Table 4. Receiver MCU pin functions.

Pin number	Name	Type	Function
1	DC-EN	Output	DC-DC converter control
2	Pow-SW	Output	Control switch
3	(R)DC-EN	-	Reserved
4	(R) Pow-SW	-	Reserved
5	CODE	Output	Feedback to transmitter
6	V-D	Input	Detect coil voltage
7	V-P1	-	Reserved
8	V-P2	-	Reserved
9	V-P3	-	Reserved
10	V-P4	-	Reserved
11	V-P5	-	Reserved
12	V-P6	-	Reserved
13	Vss	Input	Negative supply voltage (Ground)
14	Vss	Input	Negative supply voltage (Ground)
15	Vdd	Input	Positive supply voltage
16	Vdd	Input	Positive supply voltage

U3 low-dropout regulator regulates ~20V rectified input and supplies 5V for the MCU. Zener diode ZD1 is keeping stable 5.6V on MCU power input in case of sudden voltage changes.

The DC-DC (step down) converter circuit module is shown in Figure 22. It is primarily used to stabilize voltage from the rectifier, step it down and provide to the load. The rectified signal is supplied via Q4 and undesired frequencies are removed by capacitor-input filter (C13-C14). Then the ripple components are further removed by L1 common mode choke, and the supply is fed into the U2 step-down converter (Monolithic Power Systems MP38892DN-LF). U2 is a fixed 420 KHz DC-DC converter which can regulate 4.5V to 42V input voltage to any output voltage below input voltage at a 6A continuous output current and up to 95% efficiency.

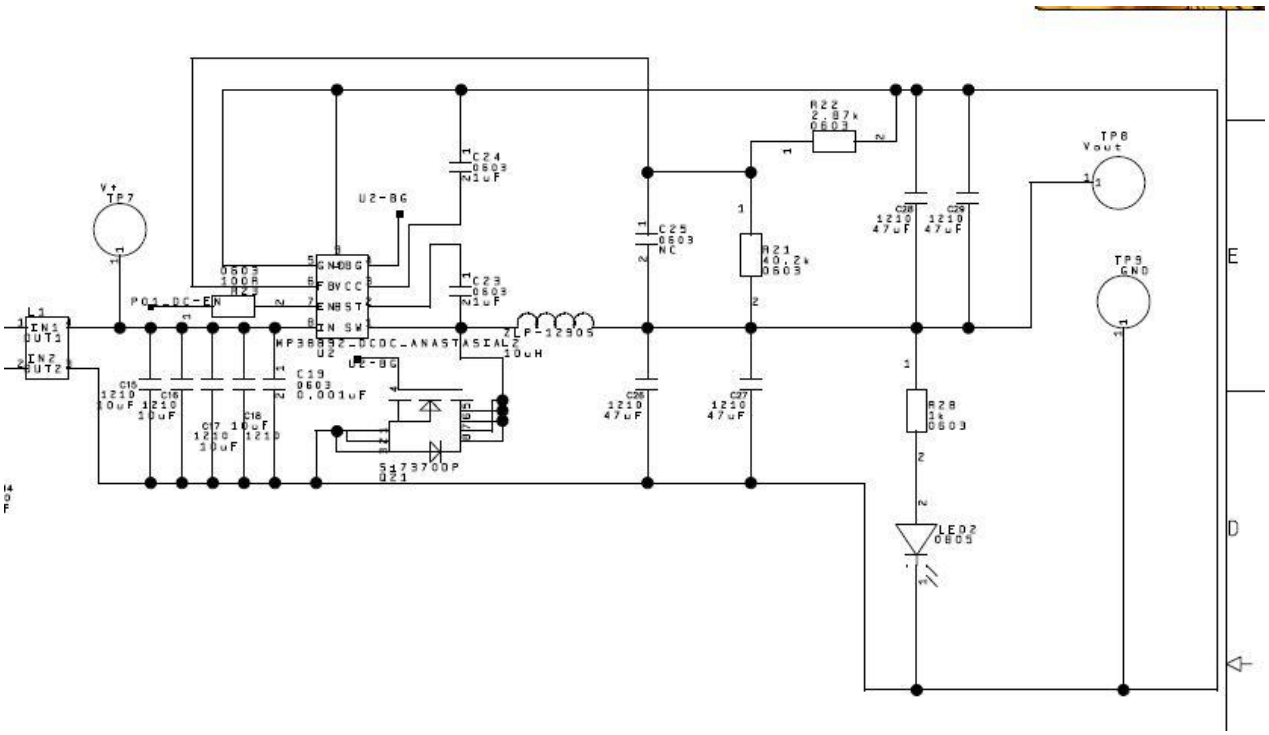

Figure 22. DC-DC converter schematic part.

The converter is controlled by the MCU pin DC-EN (normally high). The built-in synchronizable gate driver switches Q21 N-Channel MOSFET (Vishay SI7370DP-T1-E3) which is an essential part of any buck converter as well as inductor L2. The feedback pin is constantly measuring output voltage via resistor divider circuit in order to adjust its operation. The 12V output voltage is set by R21-R22 external resistor divider. Finally, LED2 indicates that the output voltage is present and the power is supplied to the load.

3.4 PCB layout design

The layout design was done in PADS Layout software, which is a part of Mentor Graphics PADS ES Suite (version 9.5).

The TX PCB size is 132 mm by 72.5 mm while the RX PCB size is 70 mm by 70 mm and both are 4-layer boards. The layers are Top, Inner layer 1, Inner layer 2 and Bottom. Figure 23 shows the layers setup dialog and all assigned settings.

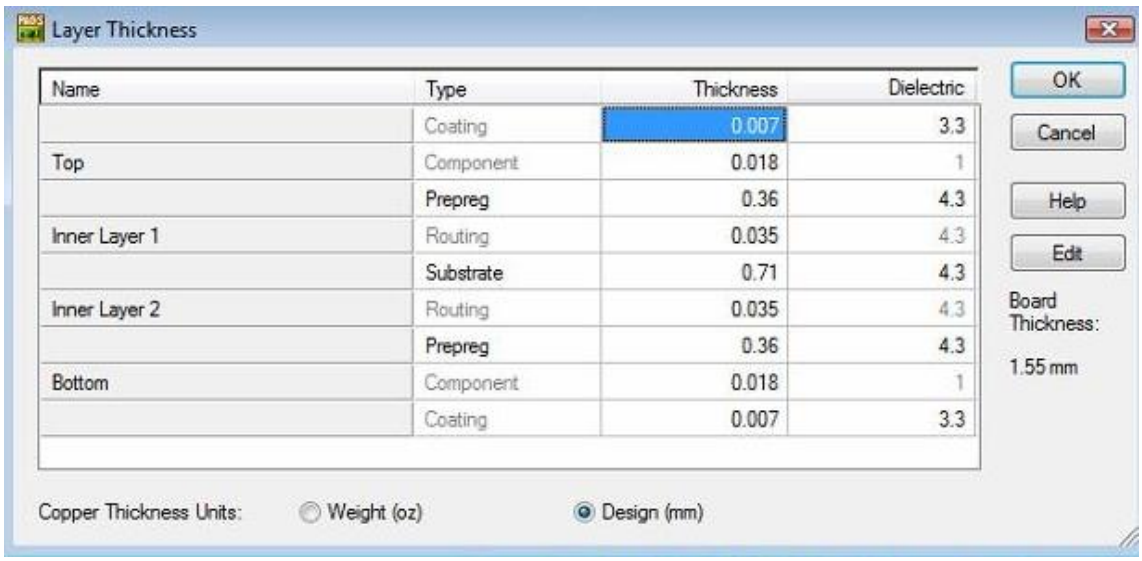

Figure 23. Transmitter and receiver PCBs layer stack.

The boards are 1.55 mm thick and mostly routed using copper planes rather than plain traces. Another important step is the design rules settings where all the clearances are set according to design requirements and manufacturer recommendations. Figure 24 illustrates the default rules setup dialog for TX (top) and RX (bottom).

TX PCB minimum trace width was 0.127 mm and maximum trace width was 2.54 mm. TX clearances for traces, vias, pads and SMDs were assigned to 0.1778 mm.

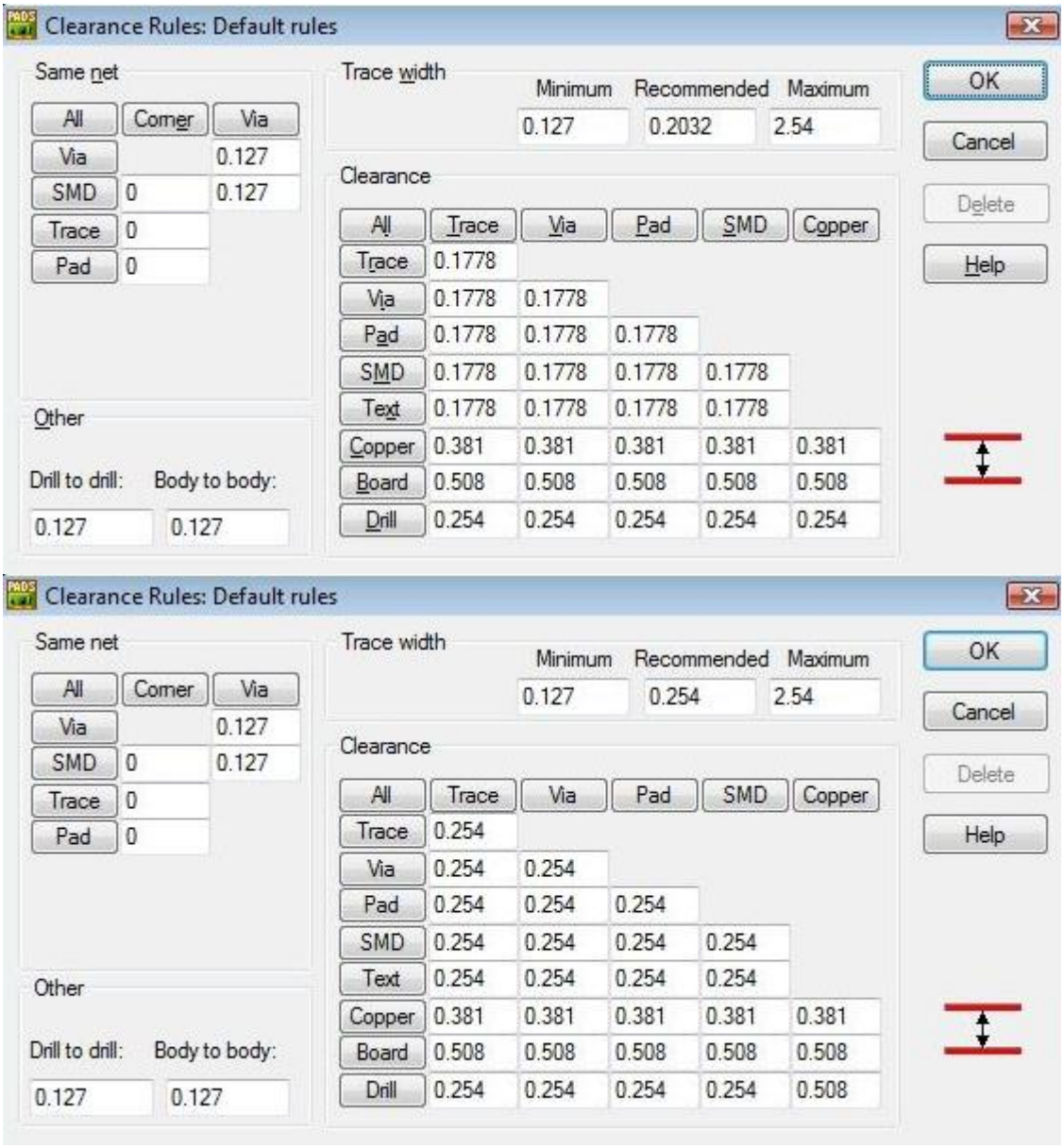

Figure 24. Transmitter (top) and receiver (bottom) default clearance rules.

RX PCB minimum trace width was 0.127 mm and maximum trace width was 2.54 mm. RX clearances for traces, vias, pads and SMDs were assigned to 0.254 mm.

After the layout was completed, Gerber files and bill of materials (BOM) were created. Gerber format is an old industrial image file format which is still used nowadays mostly by PCB manufacturers. It is used to transfer the board data from the design phase to the manufacturing phase. Gerber files contain the necessary information about each layer configuration such as solder mask, silkscreen, board outline, holes locations. Gerber files can be created with a special wizard in PADS Layout. It is necessary to mark which layers to be added to the file, as well as markings and notations since they are used by the manufacturers to produce PCB according to the specifications given.

BOM is a list of all components used in the project. It is important to keep track of each component, its name, value, part type, PCB decal, manufacturer, order code and electrical characteristics. The whole system has approximately 140 components, which have to be organized in a clear way for ordering and future development.

4 Results and discussion

4.1 Tests and measurements

After the design was completed, the necessary files were sent to the manufacturer and the PCBs were produced according to specifications. The components were ordered according to the BOMs and the PCBs were hand-soldered. The readymade transmitter and receiver modules are depicted in Figure 25.

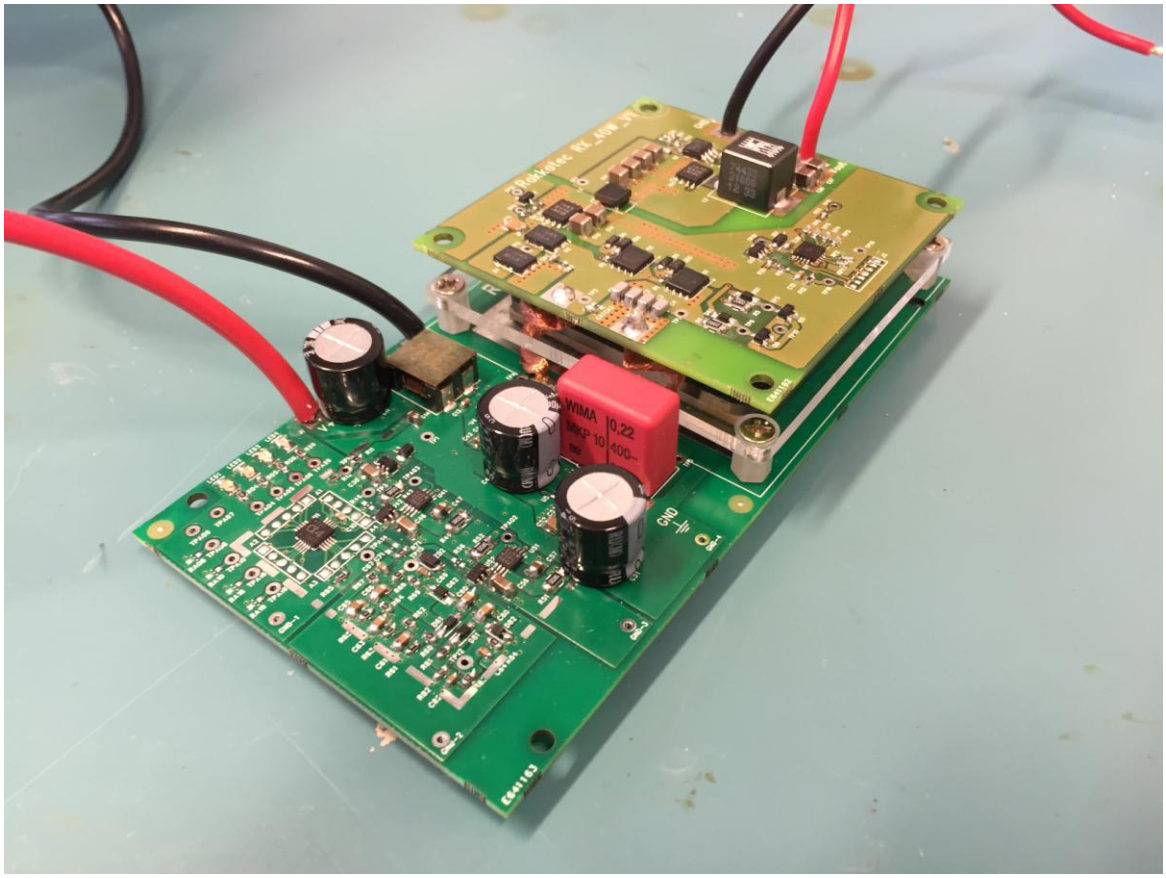

Figure 25. Custom 40W WPT system PCBs.

The system has a traditional design where transmitter electronics are located on the left side while the TX coil is located on the right side where the receiver is placed. The input and output power cables are soldered directly to the boards. Plexiglas plates can be attached to both boards in order to secure the transmission area and provide the minimum TX-RX distance.

4.1.1 Efficiency evaluation

A number of tests were done to check the operations of the system (Figure 26).

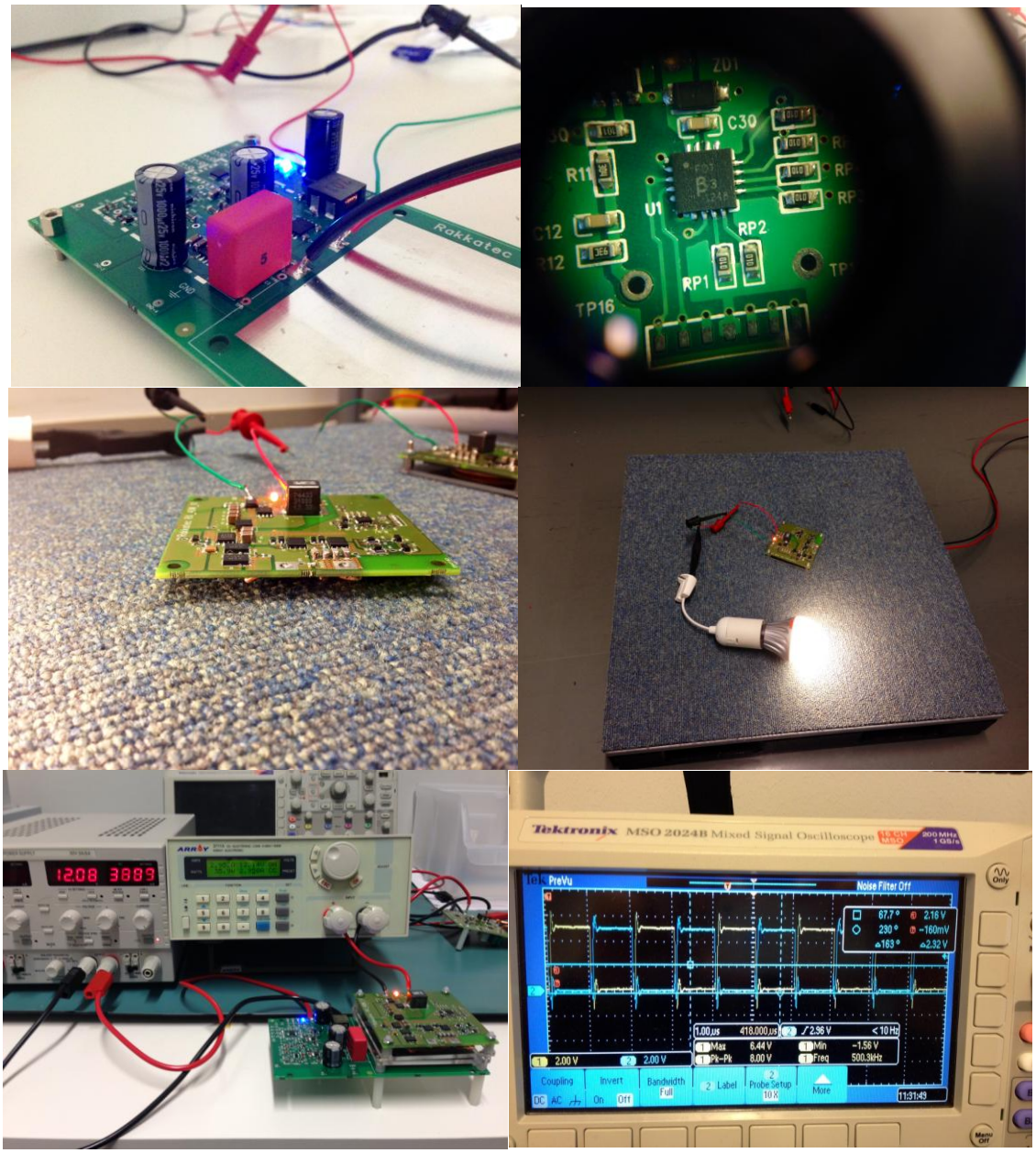

Figure 26. Custom 40W WPT system testing

Since efficiency is an important part of the system's operation, corresponding measurements were carried out. The measurement data is presented in Table 4 and the efficiency curve is shown in Figure 27.

Table 4. Custom 40W WPT system efficiency measurements data.

TX voltage, V	TX current, A	TX power, W	RX power, W	Efficiency	Load, Ohm
12,08	0,8	9,664	5	51,7384106	29,47592
12,08	1,245	15,0396	10	66,49113008	14,73796
12,08	1,71	20,6568	15	72,61531312	9,825306667
12,08	2,165	26,1532	20	76,47247756	7,36898
12,08	2,645	31,9516	25	78,24334306	5,895184
12,08	3,125	37,75	30	79,47019868	4,912653333
12,08	3,625	43,79	35	79,92692396	4,210845714
12,08	3,77	45,5416	36,4	79,92692396	4,04889011

The test was carried out using Array 3711A programmable DC electronic load. TX voltage is the voltage supplied to the transmitter module and RX power is the total power that sinks in the load on a constant current mode.

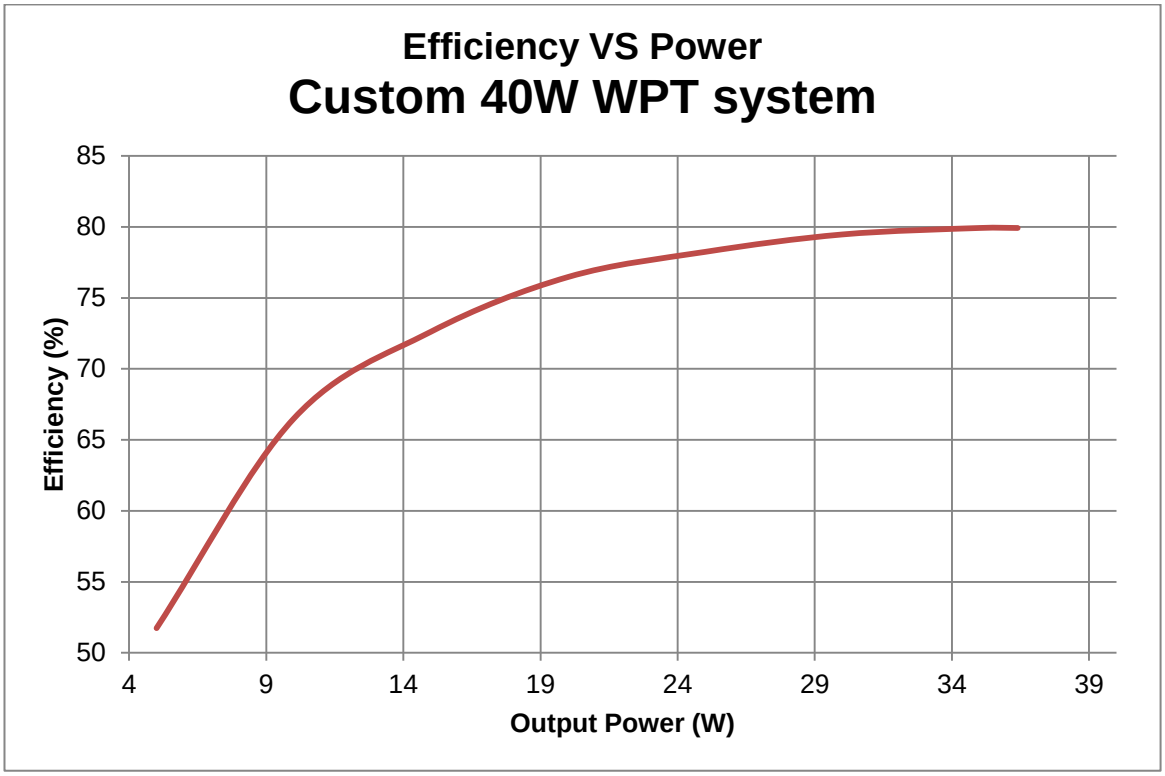

Figure 27. Custom 40W WPT system efficiency versus power.

The efficiency is growing steadily from 51% at 5W output to about 80% at 34-40W output. Hence, we can conclude that the maximum efficiency is achieved at the maximum

power load. The comparison of efficiency between a custom 40W WPT system and the TI 5W Qi kit is shown in Figure 28.

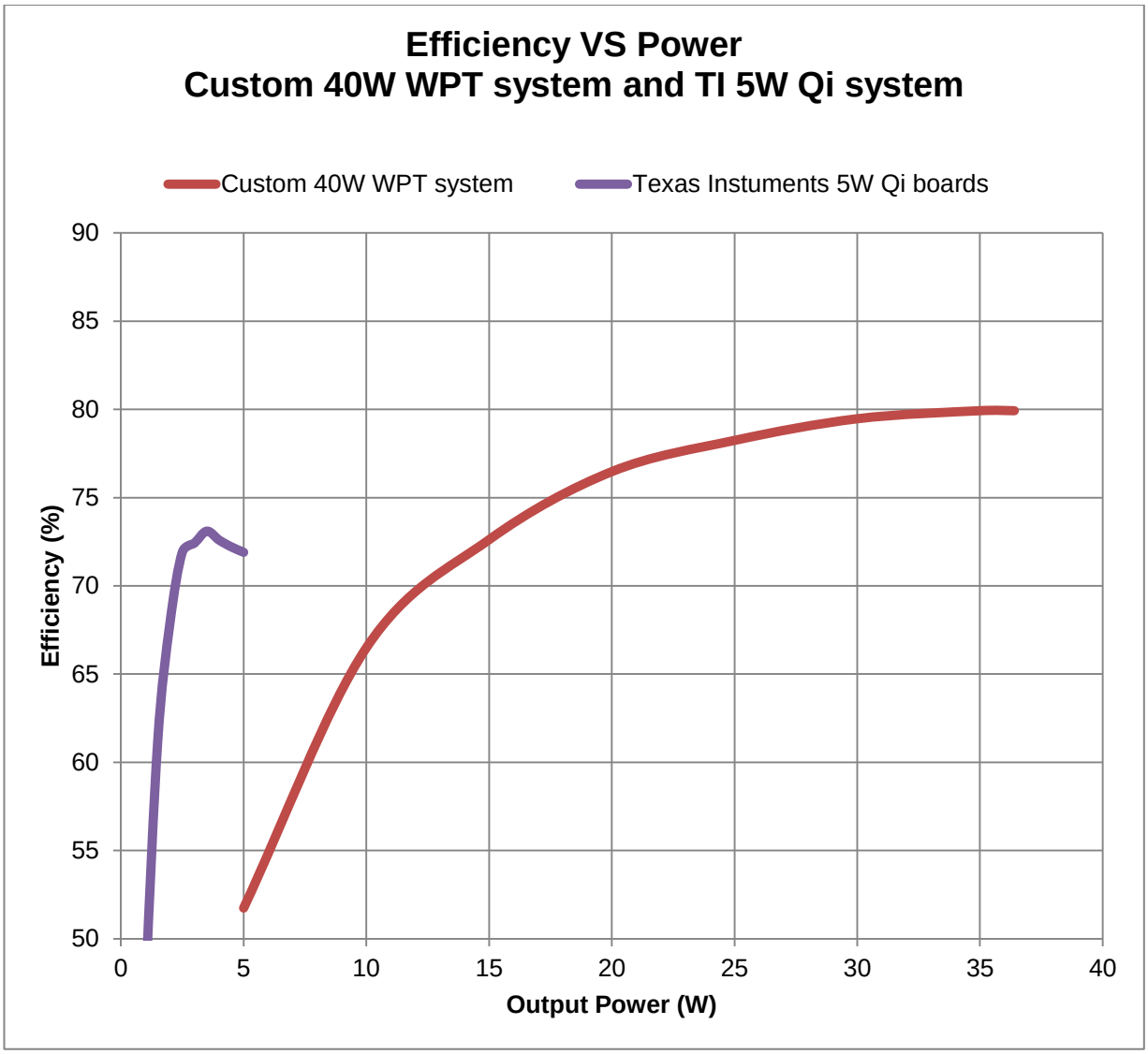

Figure 28. Custom 40W WPT system and TI 5W Qi system efficiency versus power curves.

Above all the custom 40W WPT system shows very promising results delivering up to 8 times more power (40W max) than the TI 5W Qi system with almost 10% more efficiency. Furthermore, the maximum transmission distance between the boards can reach 20 mm depending on the load, the material between the units and the alignment of the coils.

4.1.2 EMF test

In order to check if the custom 40W WPT system is safe, electromagnetic field (EMF) measurements with SPECTRAN NF5035 pre-Compliance EMC/EMI spectrum analyzer were conducted. According to the test results, 40W system's exposure at 125 kHz was below both IEEE and ICNRP limits. No critical excesses were observed. Different EMF strength values were measured in different distances to the device. The average values of EMF strength were 5.6µT without load and 6µT with the floor lamp. Obviously, the system complies even with the strict IEEE uncontrolled environment limit.

4.1.3 EMC scan

The EMC scan was performed using Detectus EMC-Scanner with a near-field probe. The receiver used in this measurement was a Rohde & Schwarz 9 kHz – 13.6 GHz spectrum analyzer. The main idea was to make comparative measurements of the intensity and the location of electromagnetic radiation sources at a component level. HP11941A close-field probe was used to track down the sources of RF emission on the PCBs in 9 kHz to 30 MHz range. The temperature scans were done using a high-resolution heat scanner and a non-contact thermometer.

Firstly, the scanner was calibrated and the probe setting was configured. After that, the pre-scan measurement was carried out on the 9 kHz to 30 MHz range (Figure 29).

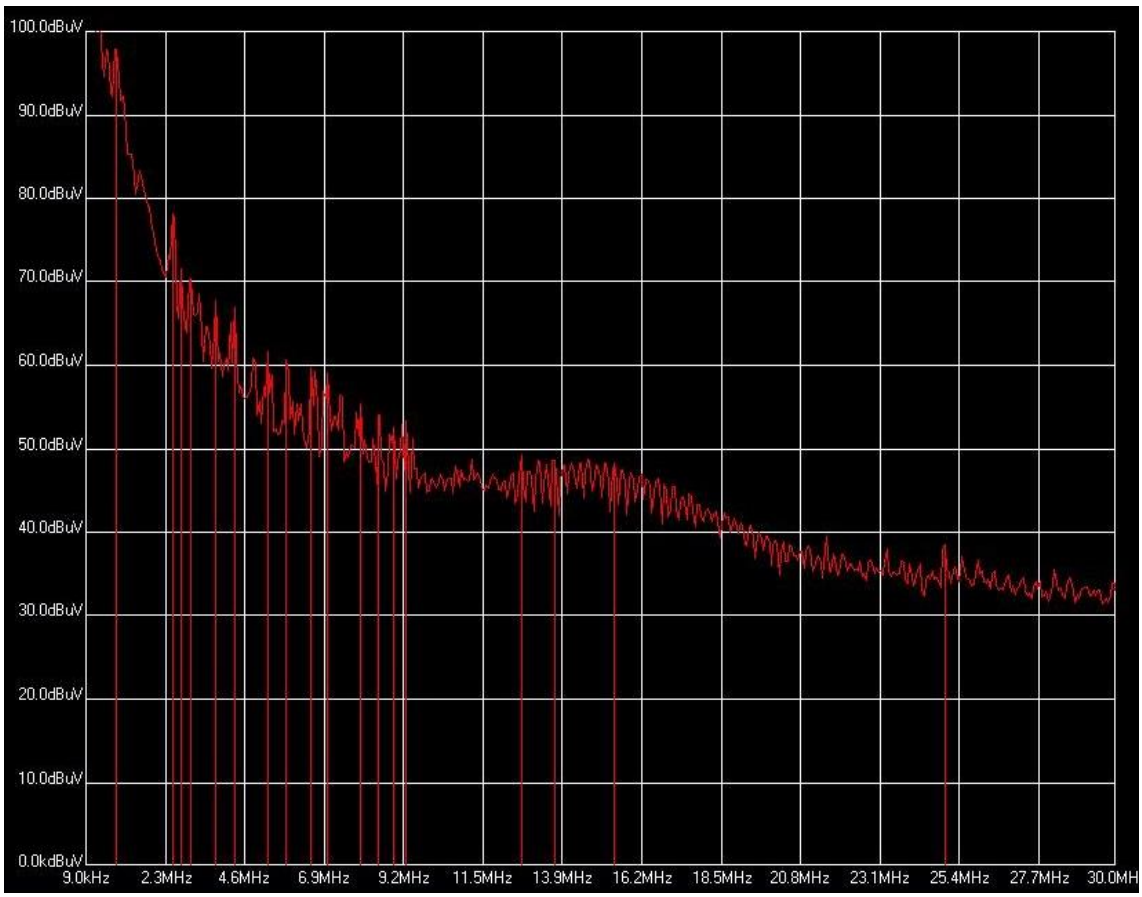

Figure 29. Pre-scan measurement result.

Measurement was done with the purpose of getting the overall idea of the frequency range and choosing the most crucial peaks for detailed evaluation. The following frequencies were chosen: 2.5 MHz and 13.6 MHz. The 2.5 MHz scan is shown in Figure 30.

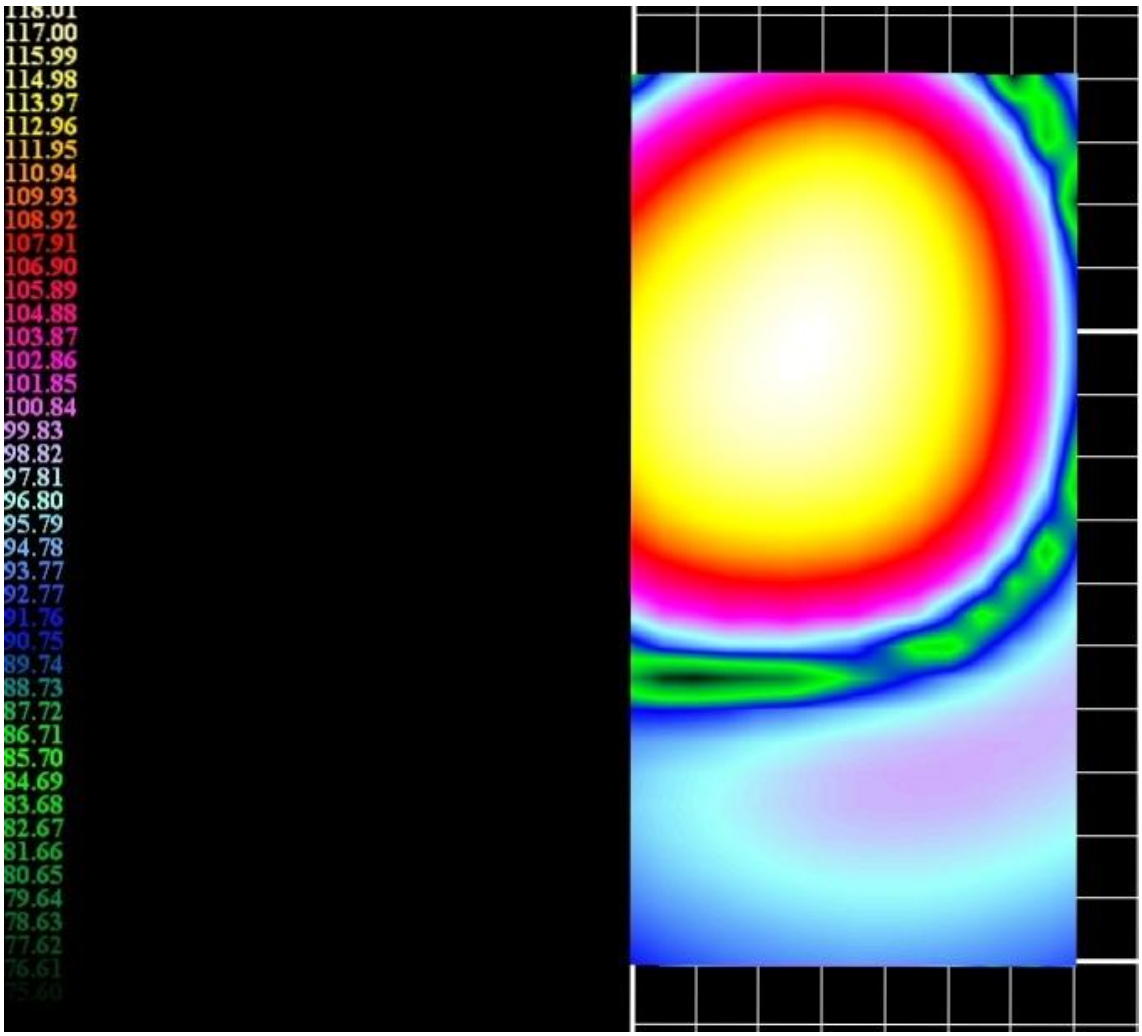

Figure 30. 2.5 MHz near-field scan.

As expected, the coil area on RX has the strongest emission up to 118 dBuV comparing to the rest of the PCB. The emission measured at 2.5 MHz was the highest compared to those on other frequencies. The 13.6 MHz scan is shown in Figure 31.

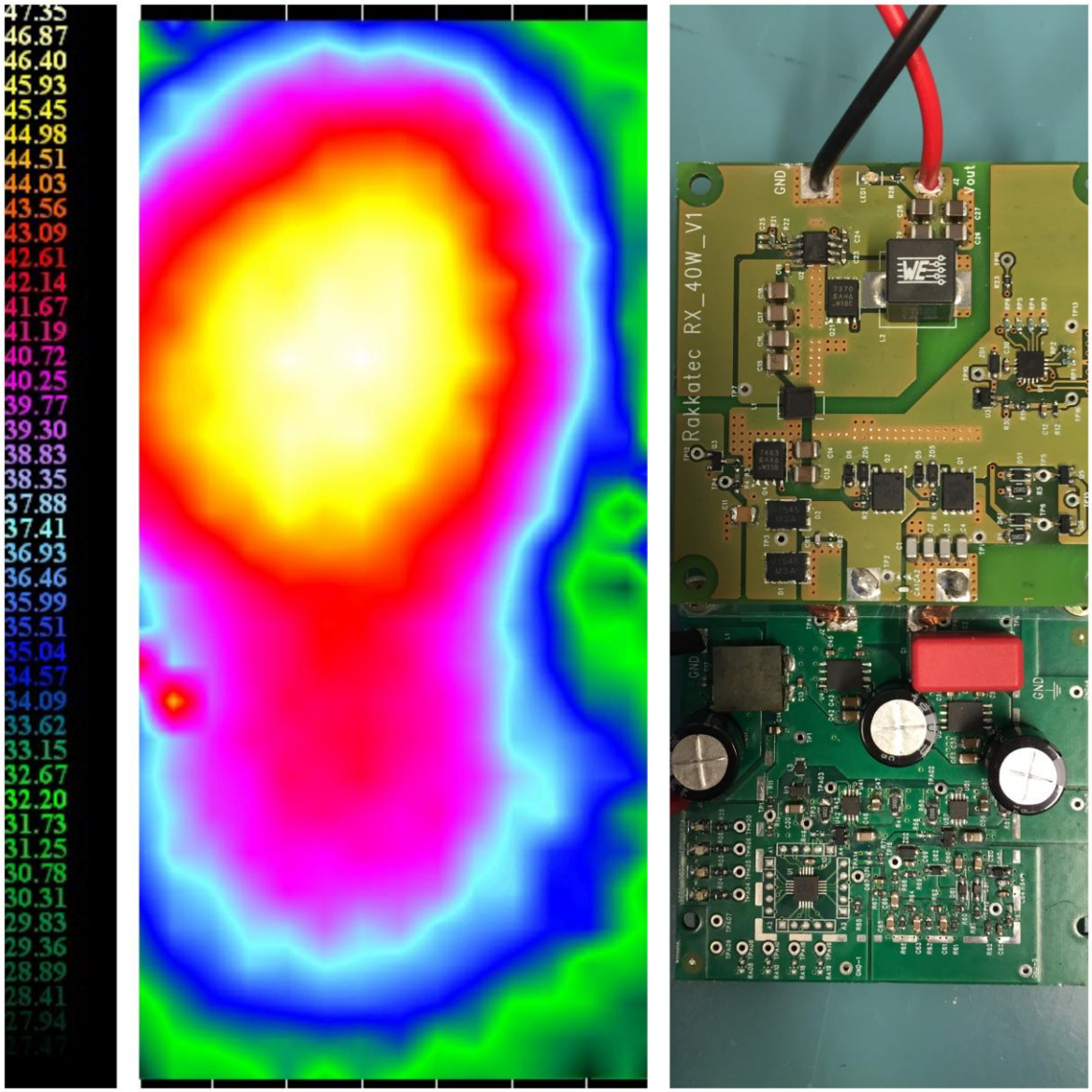

Figure 31. 13.6 MHz near-field scan.

It is clear that on 13.6 MHz the input filter inductor L1 starts to radiate as strongly as the coil and the RX board itself though the level is only 47 dBuV.

Finally, the temperature scan is depicted in Figure 32. The temperature scan was done using Thermo-Hunter Built-IN2 non-contact thermometer, which has a 0-150 °C range with +/- 0.3 °C resolution and 500 ms response time.

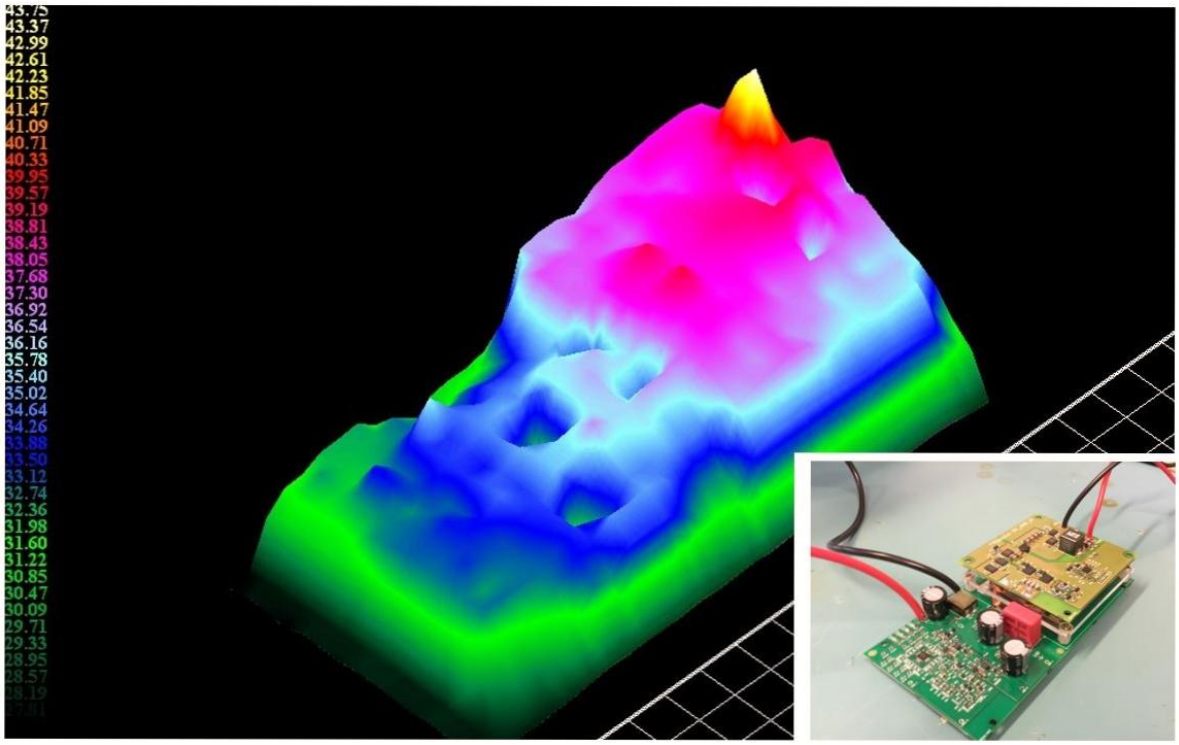

Figure 32. High-resolution 3D heat scan.

Looking at Figure 32, we may say that the highest temperature of 43°C is reached in the middle of the RX where the buck converter, inductor and the coil are located. Then the temperature gradually declines with ~40°C on the RX surface and down to ~35°C on the main transmitter parts. Surprisingly the electrolytic capacitors on TX have almost room temperature, which can be seen as 3 small cavities in the middle of the TX. Because of the measurement, we were able to localize small heat sources such as surface mounted components.

We can conclude that unexpected radiated components were not found. As was previously stated, the coil and inductor were main emission sources. It has to be said that the EMC near-field scan does not give grounds for compliance measurements with any of the standards or rules (for those we have open-air test sites (OATS) and EMC shielded room/anechoic chamber tests). These standards are specified for products or systems and not for components or elements. Instead, an EMC near-field scan provides an objective comparative perspective to find potential emission problems and locations of radiation sources at a component level.

4.2 Development of the NextFloor WPT prototypes

4.2.1 NextFloor + WPT concept

The last stage of the project was the actual integration of the wireless power transfer systems to the NextFloor flooring elements (Figure 33).

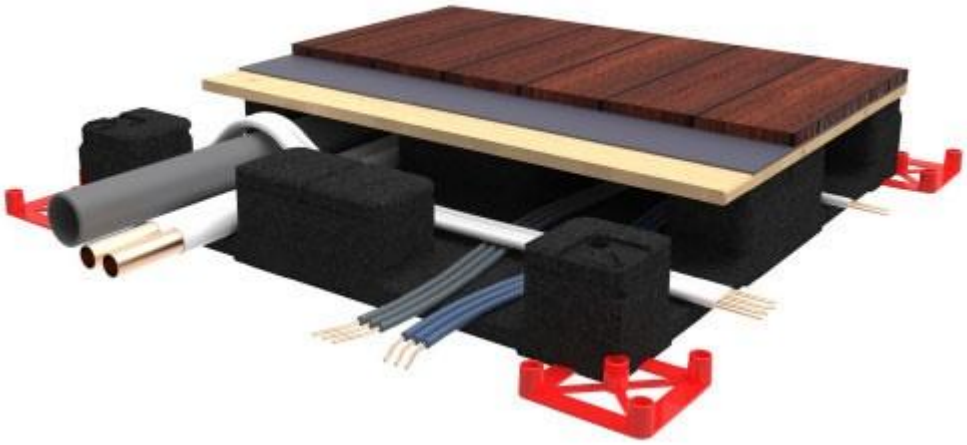

Figure 33. NextFloor element.

Nontraditional low-elevated floor segments are 50 cm by 50 cm and can have the height of 2.5 cm, 4 cm and 7 cm. A striking point is that the segment is extremely portable and can be used with different flooring materials without any complicated installation procedures. It was crucial to integrate the wireless power transfer technology into the floor system in order to make it really “smart” and innovative. Figures 34-35 represent the concept drawings of what was expected as the final product.

Figure 34. NextFloor + WPT concept picture.

The main idea of a NextFloor room is that each element of furniture has an integrated receiver unit and can be freely placed on the floor under which transmitter is located (Figure 33). In particular, an RX coil could be in the base of a floor lamp or in a table's leg or mounted in a power outlet strip. Figure 34 shows a floor lamp and a speaker concept standing on the NextFloor segments powered wirelessly.

Figure 35. NextFloor WPT floor lamp concept picture.

The important point that had to be considered was the simplicity for the end user who should easily place a lamp on the desired segment of the floor without a need to connect any cables and which at the same time could be moved to another place.

4.2.2 Qi-compatible demo-table

As a result, several prototypes were developed based on the TI 5W Qi system and the custom 40W WPT system. A Qi-compatible demo-table is illustrated in Figure 36.

Figure 36. Qi-compatible demo-table.

The Qi-compatible demo-table has two wireless charging points, which provide a 5W power output. This is enough to charge the battery of a phone, which has a special circuit, and a coil integrated inside or a special Qi-compatible case. Furthermore, the system can light up small table lamps. The crucial advantage of the system is its portability. One power cable to the main socket is needed to launch both WPT points. The transmitter unit is installed in a 3D-printed box, which perfectly fits underneath the NextFloor element. The coil holder is also 3D-printed and aligned with the floor element. The transmitter is powered via 19V plug-in power supply.

4.2.3 Non-standardized 40W WPT floor-demo

Since the custom 40W WPT system has enough power capabilities to supply any DC LED bulb integrated in floor lamps, an Ikea floor lamp was modified to work with the system. The receiver module was integrated inside the bottom part with the coil faced towards the floor in accordance with the transmitter coil under the flooring material (Figure 37).

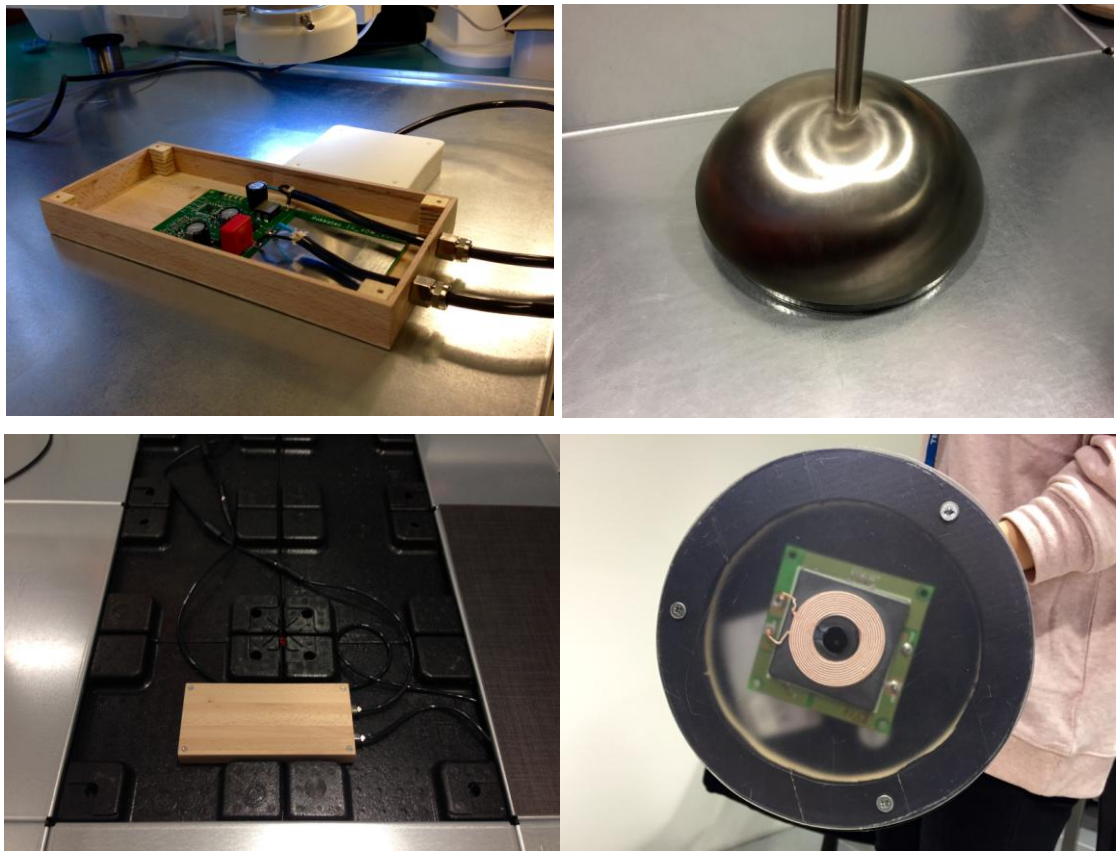

Figure 37. 40W WPT floor-demo installation.

The transmitter was placed in a handmade wooden box, which perfectly fitted underneath the segment. The coil holder was 3D printed and aligned with the floor element. The transmitter was powered via 12V plug-in power supply, which was attached via a standard connector. Two WPT spots were made to show the flexibility of the non-standardized floor-demo (Figure 38).

Figure 38. Non-standardized 40W WPT floor-demo.

The lamp can be placed at any point at any time. The only condition is to place it exactly on the marked place due to the inductive coupling requirements of full alignment. That is why it may take some time to find the correct position, but after alignment, the system will work steady and without any disruptions. It is obvious that the developed system can be integrated into a wide range of devices. The only limitation is the size and maximum power.

5 Conclusions

All aspects considered, the project had a rapid start and the wireless power concept was well proven. The goal of the project was the design and development of the wireless energy transmission system prototype and its implementation in the NextFloor innovative floor. I started by researching the relevant theoretical background and industry situation, continued with evaluation of existing products and finally proceeded with a custom WPT system and its integration into Next Floor's ingenious flooring system.

The main steps of the project were to study the physics behind wireless electricity transfer technologies, review the current industry situation and evaluate available solutions. The major objective included the design of the actual PCBs, assembly and testing and development of original prototypes. As a result, the system, consisting of a transmitter and receiver boards, was developed and it uses an inductive coupling method in order to transfer electricity wirelessly. Finally, the unique prototypes, a Qi standard compatible demo-table and non-standardized wireless power floor-demo, were designed to work together with the NextFloor ingenious flooring system.

Apparently, the project is still on-going and there are still many goals to accomplish. The next steps could include the developing of more powerful systems which could be used with laptops, their testing and debugging and integration to NextFloor via novel prototypes. Furthermore, an essential goal for future would be R&D of the magnetic resonance WPT systems, which are slowly starting to emerge and offer numerous advantages over inductive coupling transfer.

References

1. Nikola Tesla. The transmission of electrical energy without wires. Selected Tesla writings [online]. Electrical World and Engineer, 1904.
   URL: http://www.tfcbooks.com/tesla/1904-03-05.htm
   Accessed 20 September 2014.

2. Garnica, J.; Dept. of Electr. & Comput. Eng., Univ. of Florida, Gainesville, FL, USA; Chinga, R.A.; Jenshan Lin. Wireless Power Transmission: From Far Field to Near Field [online]. Proceedings of the IEEE (Volume: 101, Issue: 6); 4 April 2013, 1321-1331.
   URL:http://ieeexplore.ieee.org.ezproxy.metropolia.fi/stamp/stamp.jsp?tp=&arnumber=6494253
   Accessed 2 October 2014.

3. Brown, William C. The History of Power Transmission by Radio Waves [online]. Microwave Theory and Techniques, IEEE Transactions on (Volume: 32, Issue: 9); September 1984, 1230-1242.
   URL:http://ieeexplore.ieee.org.ezproxy.metropolia.fi/stamp/stamp.jsp?tp=&arnumber=1132833
   Accessed 13 October 2014.

4. Van Wageningen, D. ; Solid State Lighting, Philips Res. Eur., Aachen, Germany; Staring, T. The Qi wireless power standard [online]. Power Electronics and Motion Control Conference (EPE/PEMC), 2010 14th International; 6-8 September 2010, S15-25 - S15-32.
   URL:http://ieeexplore.ieee.org.ezproxy.metropolia.fi/stamp/stamp.jsp?tp=&arnumber=5606673
   Accessed 28 September 2014.

5. Tseng, R. ; Qualcomm Technol., Inc., San Diego, CA, USA ; von Novak, B. ; Shevde, S. ; Grajski, K.A. Introduction to the alliance for wireless power loosely-coupled wireless power transfer system specification version 1.0 [online]. Wireless Power Transfer (WPT), 2013 IEEE; 15-16 May 2013, 79–83.
   URL:http://ieeexplore.ieee.org.ezproxy.metropolia.fi/stamp/stamp.jsp?tp=&arnumber=6556887
   Accessed 5 October 2014.

6. Grajski, K.A. ; Qualcomm Inc., San Diego, CA, USA ; Tseng, R. ; Wheatley, C. Loosely-coupled wireless power transfer: Physics, circuits, standards [online]. Microwave Workshop Series on Innovative Wireless Power Transmission: Technologies, Systems, and Applications (IMWS), 2012 IEEE MTT-S International; 10-11 May 2012, 9-14.
URL:http://ieeexplore.ieee.org.ezproxy.metropolia.fi/stamp/stamp.jsp?tp=&arnumber=6215828
Accessed 10 October 2014.

7. Mark Estabrook. The convenience of wireless charging: It's just physics. White paper [online]. MediaTek, 2013.
URL: http://cdn-cw.mediatek.com/Mediatek_Wireless_Charging.pdf
Accessed 30 August 2014.

8. Morris Kesler. Highly Resonant Wireless Power Transfer: Safe, Efficient, and over Distance. White Paper [online]. WiTricity Corporation, 2013.
URL: http://www.witricity.com/assets/highly-resonant-power-transfer-kesler-witricity-2013.pdf
Accessed 19 August 2014.

9. Sun, Tianjia, Xie, Xiang, Wang, Zhihua. Wireless Power Transfer for Medical Microsystems [eBook]. New York: Springer; 2013.
URL: http://www.springer.com/engineering/circuits+%26+systems/book/978-1-4614-7701-3
Accessed 1 October 2014.

10. Mark I. Montrose, Edward M. Nakauch.Testing for EMC Compliance: Approaches and Techniques. Canada: Wiley-IEEE Press; 2004.

11. Matias, R.; Cunha, B.; Martins, R. Modelling inductive coupling for Wireless Power Transfer to integrated circuits [online]. Wireless Power Transfer (WPT), 2013 IEEE; 15-16 May 2013, 198–201.
URL:http://ieeexplore.ieee.org.ezproxy.metropolia.fi/stamp/stamp.jsp?tp=&arnumber=6556917
Accessed 5 November 2014.

12. Qi Wireless Power Consortium. Wireless Power Technology [online].
URL: http://www.wirelesspowerconsortium.com/technology/
Accessed 1 August 2014.

13. Cincinnati Technical Center. Electromagnetic radiation and how it affects your instruments [online]. Occupational Safety & Health Administration. Cincinnati, Ohio; May 20, 1990.
URL: https://www.osha.gov/SLTC/radiofrequencyradiation/electromagnetic_fieldmemo/electromagnetic.html#section_6
Accessed 20 November 2014.

14. Richard Wolfson. Essential University Physics: Volume 2 (Second Edition). Harlow: Pearson Education Limited; 2014.

15. Alliance for Wireless Power Rezence [online].
URL: http://www.rezence.com/
Accessed 5 January 2015.

16. Power Matters Alliance [online].
URL: http://www.powermatters.org/
Accessed 7 January 2015.

17. Niranjan Pathare. A global wireless power standard will open the market, encourage consumers to live without power cords. White Paper [online]. Texas Instruments, 2013.
URL: http://www.ti.com/lit/wp/slyy036/slyy036.pdf
Accessed 11 January 2015.

18. Ryan Sanderson, The World Market for Wireless Power –2014 Edition [online], IHS Technology, 2014.
URL: https://technology.ihs.com/438315/wireless-power-2014.
Accessed 12 January 2015.

19. Farouk Balouchi, Bob Gohn, Wireless Power Mobile Devices, Consumer Electronics, Industrial Devices, Wireless Power Infrastructure, and Wireless Charging of Electric Vehicles: Technology Analysis, Environmental Impact, and Market Forecasts, Research report [online], Pike Research, 2012.

URL: http://www.navigantresearch.com/wordpress/
wp-content/uploads/2012/07/WPOW-12-Executive-Summary.pdf
Accessed 12 January 2015.

20. Texas Instruments power management portal [online].
URL: http://www.ti.com/lsds/ti/power-management/
wireless-power-receiver-solutions-overview.page
Accessed 29 August 2014.